Supporting information for: Structural diversity and solvent-induced transformations of a copper-based metal-organic framework with highly aromatic ligand

Abigail Edwards, Landon J. Elkins, Carla Slebodnick, Jinglei Wang, Qiang Zhang, and Tegan A. Makal

Table of Contents

Section	Content	Contains Figure	Page Range
A	Ligand Synthesis	N/A	S3 – S4
B	NMR Spectra	S1-S16	S5 – S12
C	Overview of MOF Synthesis	S17-S19	S13 – S14
D	Single-Crystal X-ray Experimental	N/A	S15-S17
E	MOF Structures	S20-S26	S18-25
F	PXRD Data	S27-S33	S26-S33
G	TGA Data	S34	S34
H	Experimental gas Adsorption Isotherms	S35-S36	S35-S36
I	IR Spectra	S37-S38	S37-S38
J	References	N/A	S39

A. Ligand Synthesis

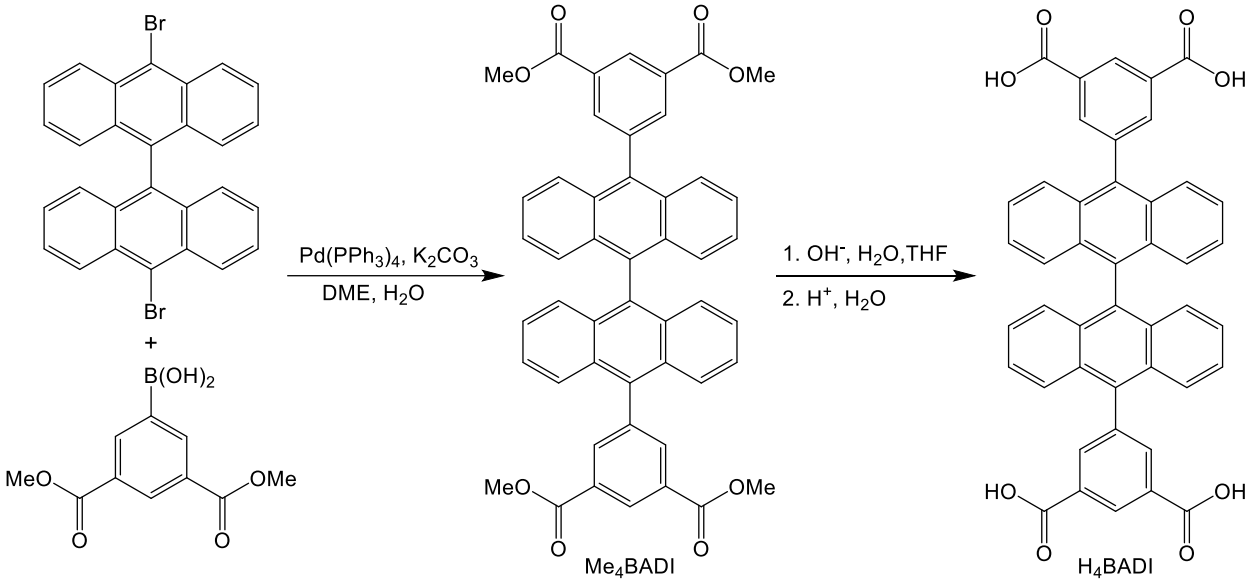

Synthesis of tetramethyl 5,5′-([9,9′-bianthracene]-10,10′-diyl)diisophthalate (Me_4BADI) To a 100-mL Schlenk flask equipped with magnetic stirrer was added 10,10′-dibromo-9,9′-bianthryl (1.998 g, 3.90 mmol), 3,5-bis(methoxycarbonyl)phenylboronic acid (3.718 g, 13.35 mmol), tetrakis(triphenylphosphine)palladium(0) (0.68 g, 0.59 mmol) and potassium carbonate (1.70 g, 12.3 mmol). The flask was purged and backfilled with argon three times before an argon-purged mixture of toluene, ethanol, and water (15:10:5 mL) was added via cannula. The rubber septum was replaced with reflux condenser, and the reaction mixture was heated at reflux under argon with stirring for six days. The organic solvent was then removed via rotary evaporator and the aqueous phase extracted with chloroform, dried over magnesium sulfate, filtered, and reduced in vacuo. The resultant solid was washed with acetone until the washings were colorless yielding a light-yellow solid that was subsequently dried in air (2.497 g, 87% yield). Found: C, 78.98; H, 4.89. Calc. for $C_{48}H_{34}O_8$: C, 78.04; H, 4.64%. ^{1}H NMR (400 MHz, $CDCl_3$): δ (ppm) 8.97 (t, 2H, J = 1.6 Hz), 8.53 (d, 4H, J = 1.6 Hz), 7.67 (m, 4H), 7.37 (m, 4H), 7.27 (m, 4H), 7.24 (m, 4H), 4.01 (s, 12H). ^{13}C NMR (100 MHz, $CDCl_3$): δ (ppm) 166.25, 140.00, 136.72, 135.27, 134.14, 131.28, 131.21, 130.18, 129.97, 127.22, 126.53, 125.93, 125.84, 52.55.

Synthesis of 5,5′-([9,9′-bianthracene]-10,10′-diyl)diisophthalic acid (H_4BADI) To a 100-mL round-bottomed flask was added Me_4BADI (2,497 g, 3.38 mmol) to a solution of potassium hydroxide (1.6 g in 40 mL THF/water, 1/1 v/v). The suspension was heated at reflux with stirring in air for 24 hours. The mixture was then cooled and filtered to remove black precipitate and THF removed via rotary evaporator. Aqueous HCl (10%) was then added to the resultant aqueous solution to precipitate H_4BADI as a yellow solid, which was subsequently collected via vacuum filtration, washed with water, and dried in air at 110 °C (2.286 g, 99% yield). Found: C, 76.37; H, 4.06. Calc. for $C_{44}H_{26}O_8$: C, 77.41; H, 3.84%. ^{1}H NMR (400 MHz, DMSO-d^6): δ (ppm) 13.50 (s, 4H), 8.76 (t, 2H, J = 1.6 Hz), 8.38 (d, 4H, J = 1.6 Hz), 7.65 (d, 4H, J = 8.8 Hz), 7.47 (m, 4H), 7.28 (m, 4H), 7.15 (d, 4H, J = 8.8 Hz). ^{13}C NMR (100 MHz, DMSO-d^6): δ (ppm) 166.60, 139.02, 135.70, 135.36, 133.35, 132.19, 130.68, 129.55, 129.43, 126.68, 126.33, 126.27, 126.21.

Synthesis of tetramethyl 5,5′-([1,1′-binaphthalene]-4,4′-diyl)diisophthalate (Me_4BNDI) To a 100-mL Schlenk flask was added 4,4′-dibromo-1,1′-binaphthalene (1.609 g, 3.90 mmol), 3,5-bis(methoxycarbonyl)phenylboronic acid (3.740 g, 15.71 mmol), tetrakis(triphenylphosphine)palladium(0) (0.68 g, 0.59 mmol), and potassium carbonate (1.60 g, 11.7 mmol). The flask was evacuated and backfilled with argon three times. A mixture of toluene/ethanol/water (15/10/5 mL) was bubbled with argon and then transferred to the reaction flask via cannula. The reaction mixture was heated at reflux with stirring for five days. The organic solvent was then removed via rotary evaporator and the aqueous phase extracted with chloroform, dried over magnesium sulfate, filtered, and reduced in vacuo. The resultant solid was washed with acetone until the washings were colorless yielding a white solid that was subsequently dried in air (2.091 g, 84% yield).

Synthesis of 5,5′-([1,1′-binaphthalene]-4,4′-diyl)diisophthalic acid (H_4BNDI) To a 100-mL round-bottomed flask was added Me_4BNDI (2.091 g, 3.24 mmol) to a solution of potassium hydroxide (1.6 g in 40 mL THF/water, 1/1 v/v). The suspension was heated at reflux with stirring in air for 24 hours. The mixture was then cooled and filtered to remove black precipitate and THF removed via rotary evaporator. Aqueous HCl (10%) was then added to the resultant aqueous solution to precipitate H_4BNDI as a yellow solid, which was subsequently collected via vacuum filtration, washed with water, and dried in air at 110 °C (1.660 g, 87% yield).

B. NMR Spectra

Me_4BADI ^1H NMR

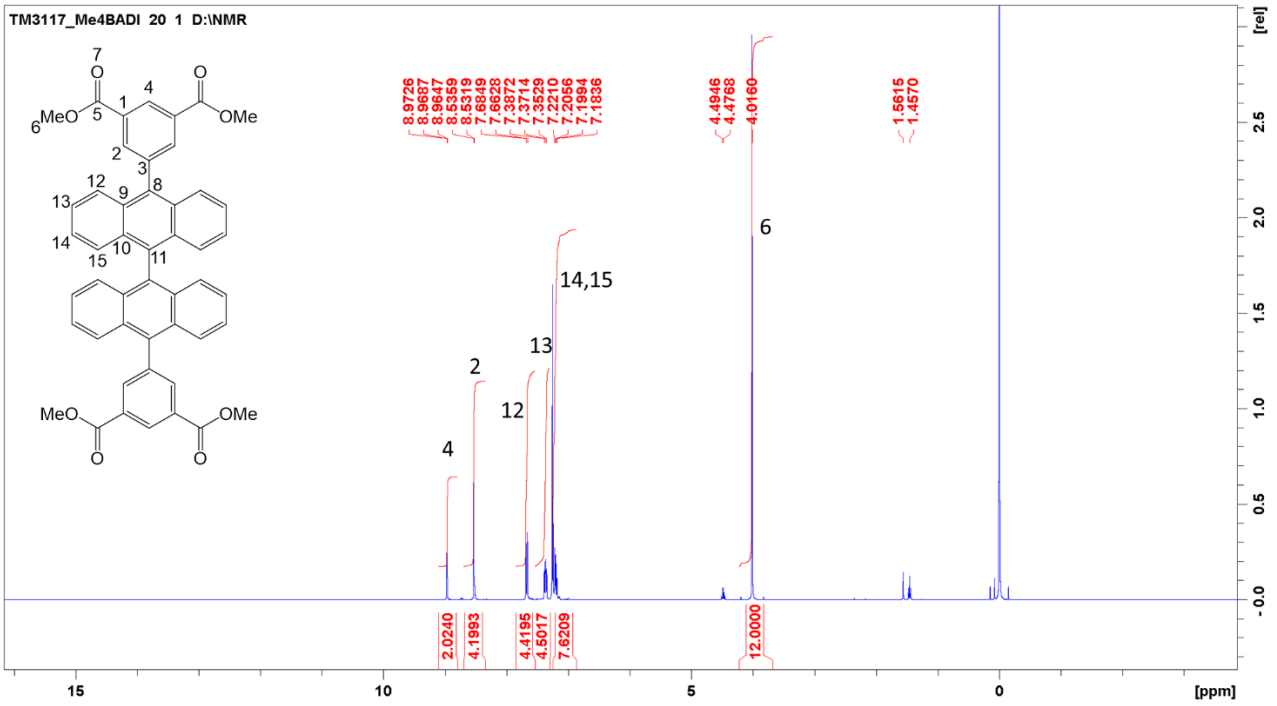

Figure S1 ^1H NMR spectrum (full-range) of Me_4BADI in $CDCl_3$

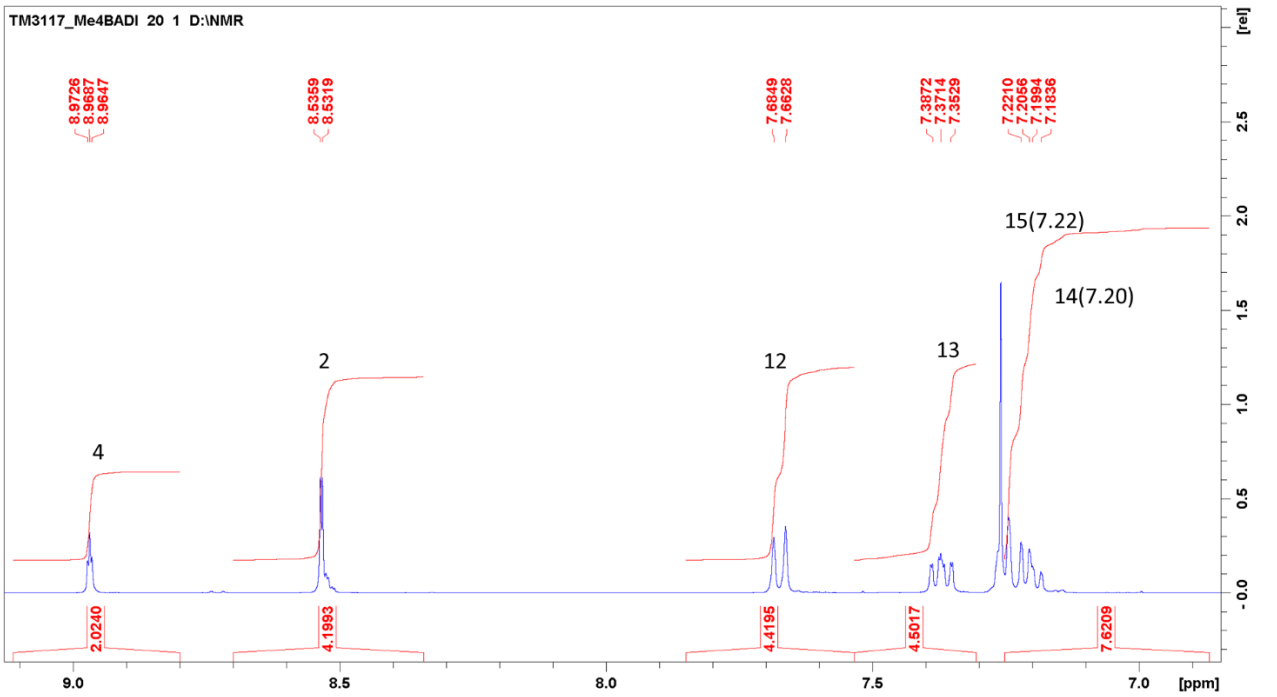

Figure S2 ^1H NMR spectrum (zoom) of Me_4BADI in $CDCl_3$

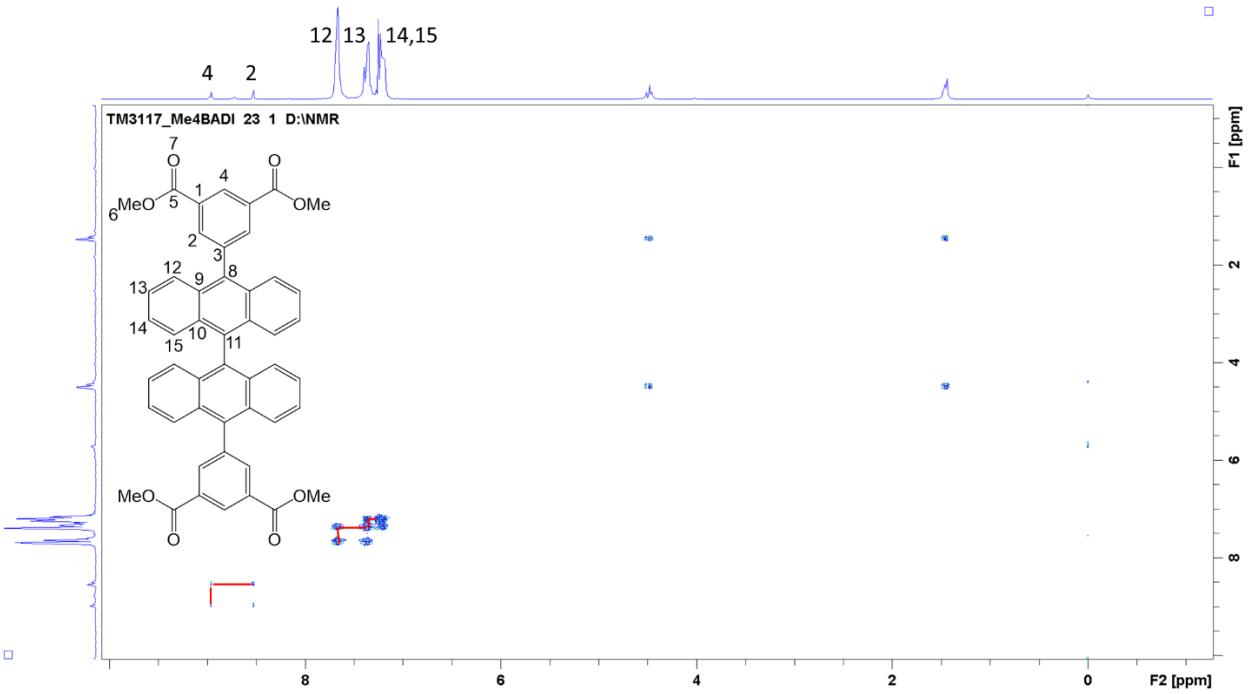

Figure S3 ^{1}H-^{1}H COSY spectrum of Me_4BADI in $CDCl_3$

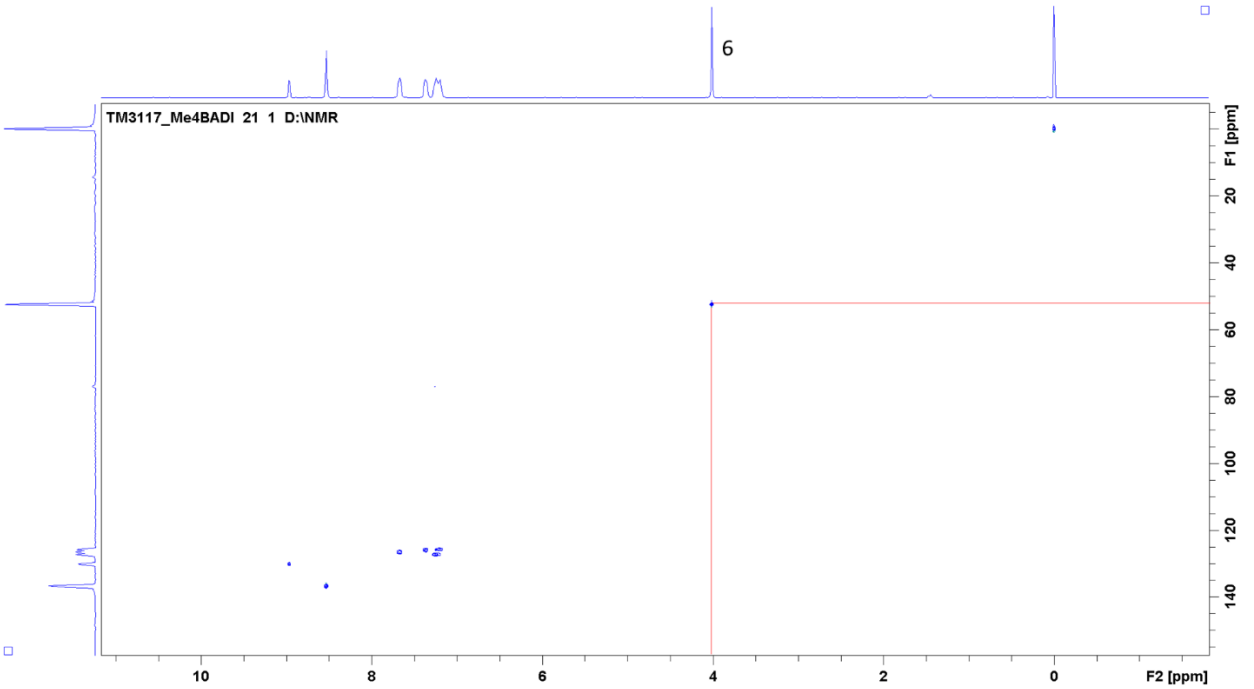

Figure S4 ^{1}H-^{13}C HSQC spectrum (full range) of Me_4BADI in $CDCl_3$

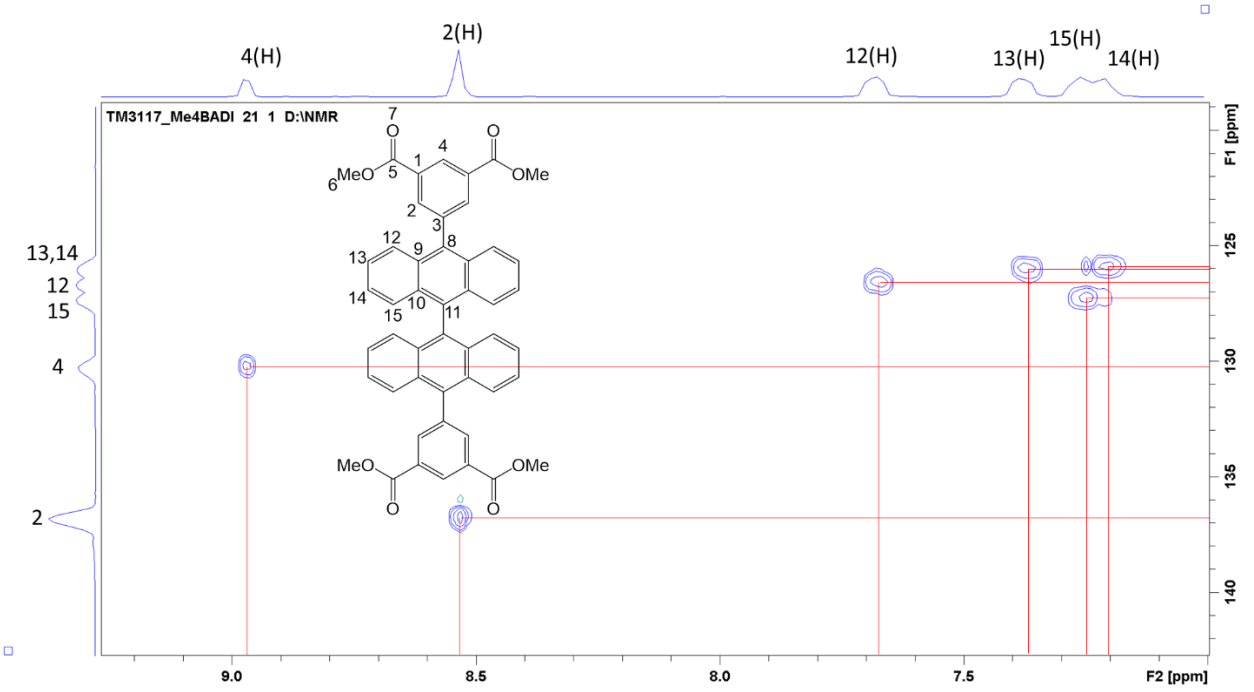

Figure S5 ^{1}H-^{13}C HSQC spectrum (zoom) of Me_4BADI in $CDCl_3$

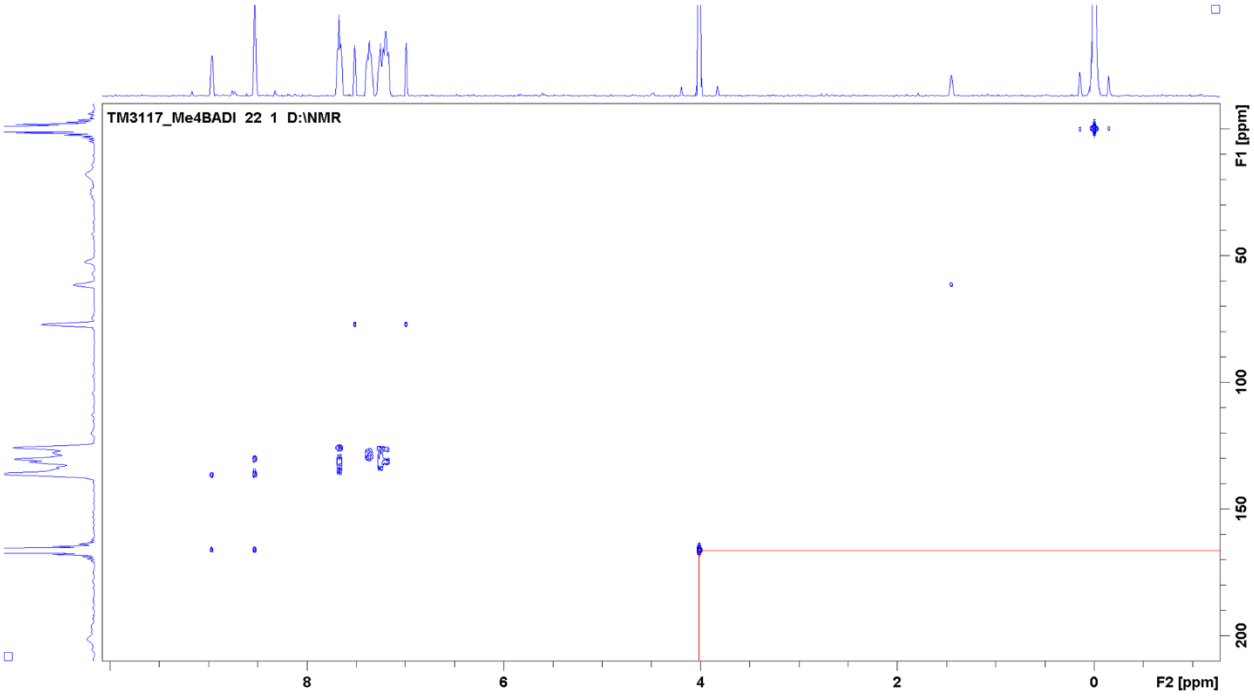

Figure S6 ^{1}H-^{13}C HMBC spectrum (full range) of Me_4BADI in $CDCl_3$

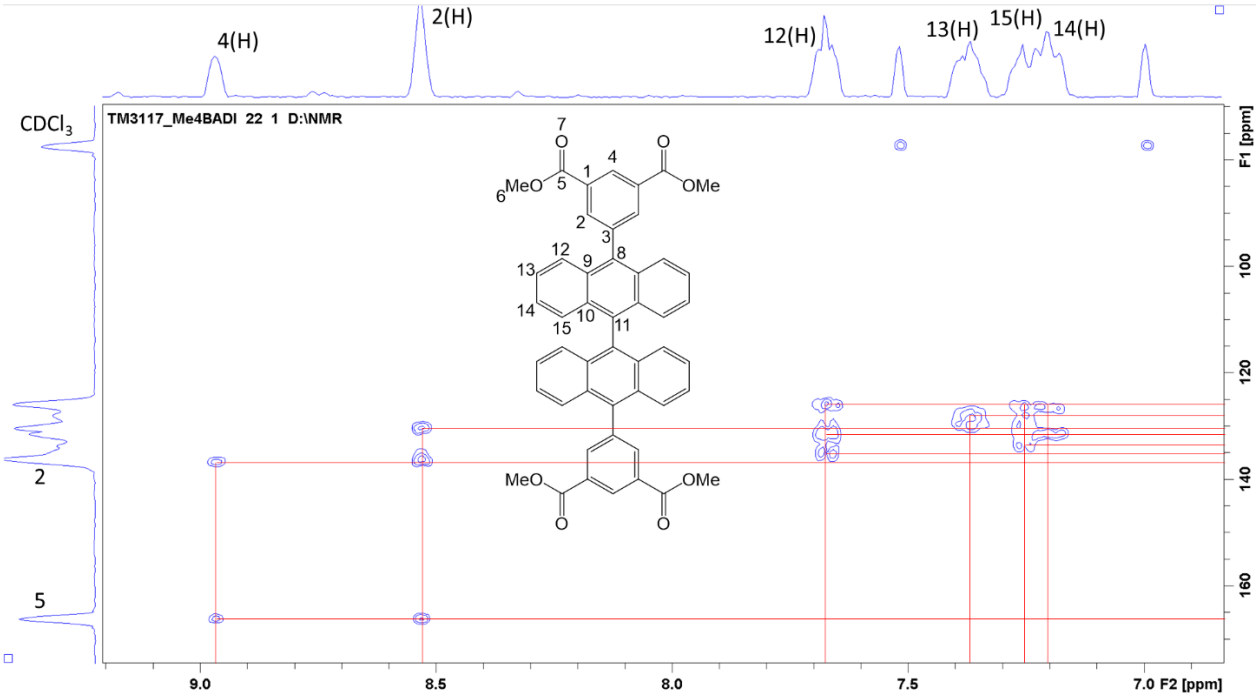

Figure S7 ^{1}H-^{13}C HMBC spectrum (zoom) of Me_4BADI in $CDCl_3$

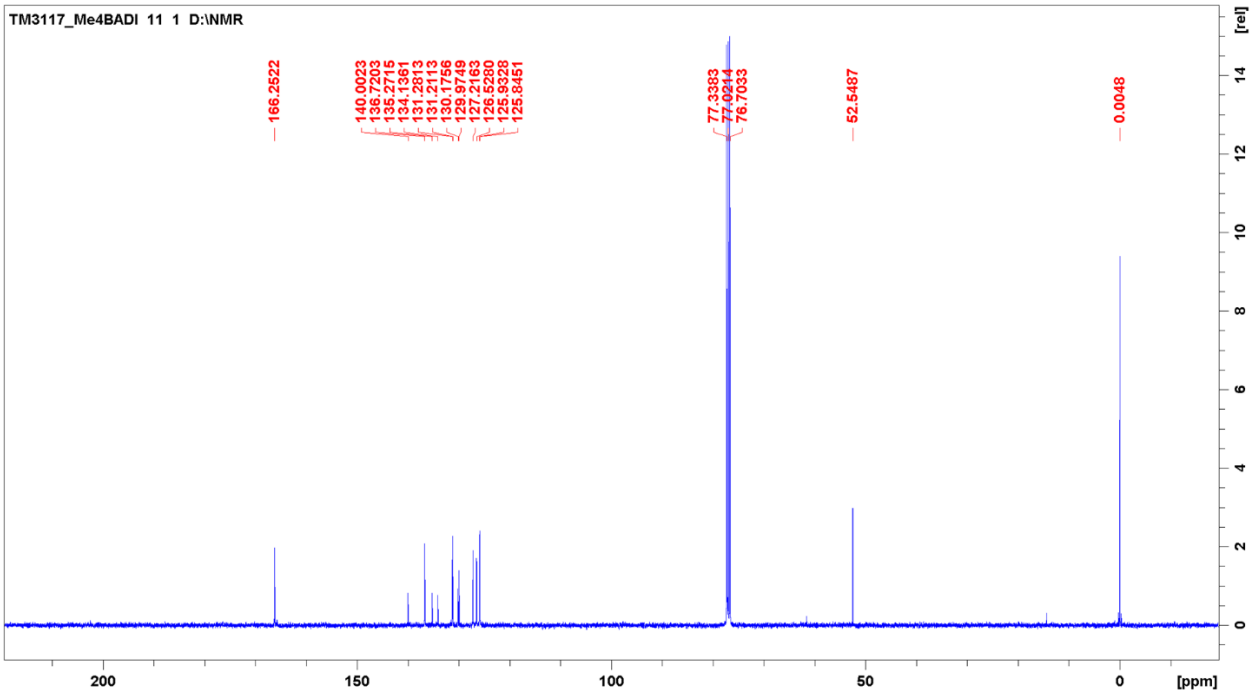

Figure S8 ^{13}C spectrum of Me_4BADI in $CDCl_3$

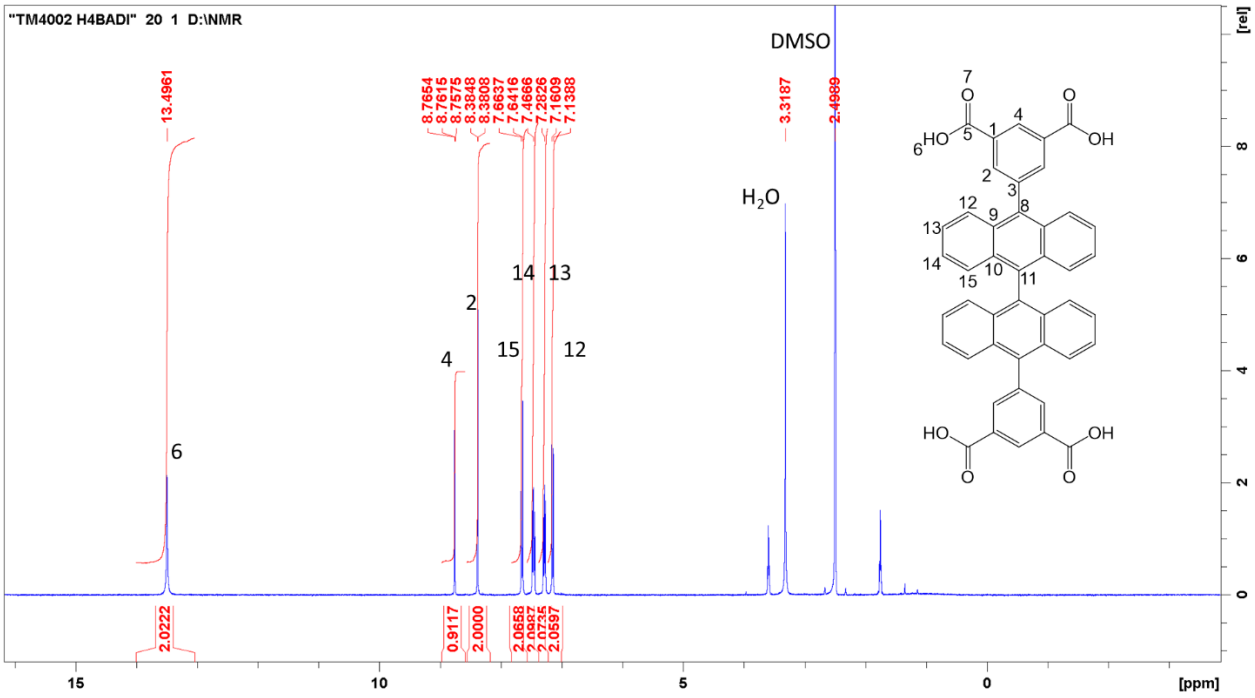

Figure S9 ^{1}H NMR spectrum (full-range) of H_4BADI in DMSO-d_6

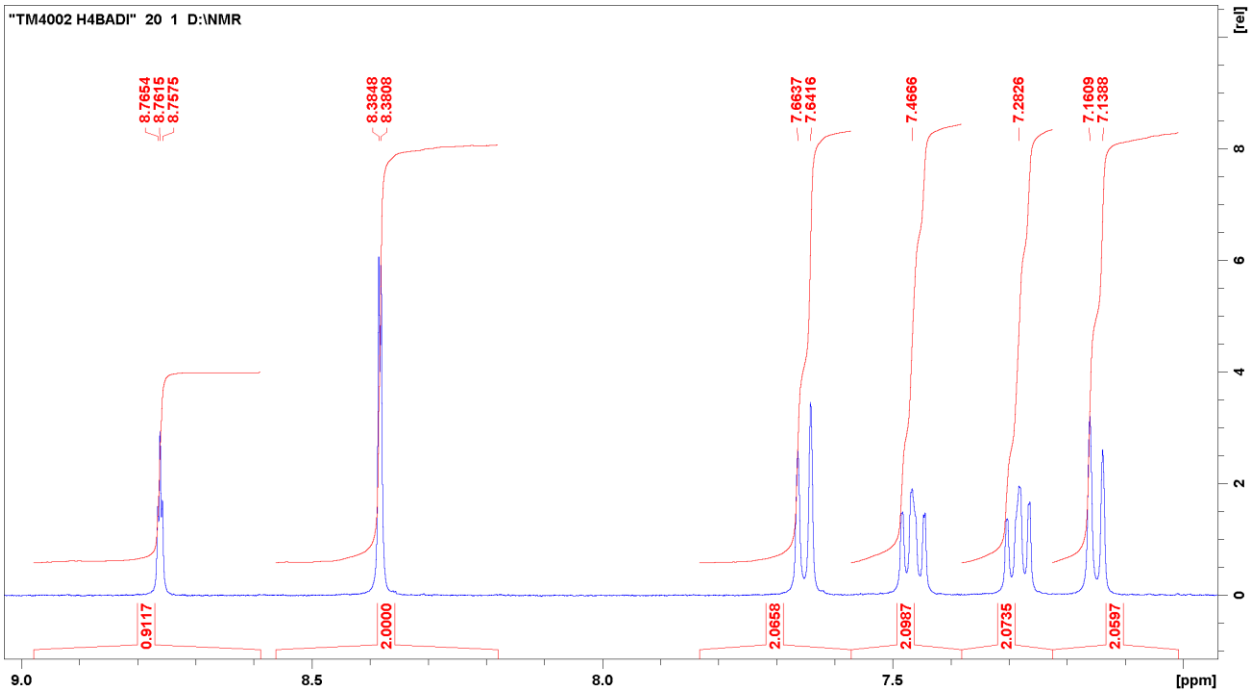

Figure S10 ^{1}H NMR spectrum (zoom) of H_4BADI in DMSO-d_6

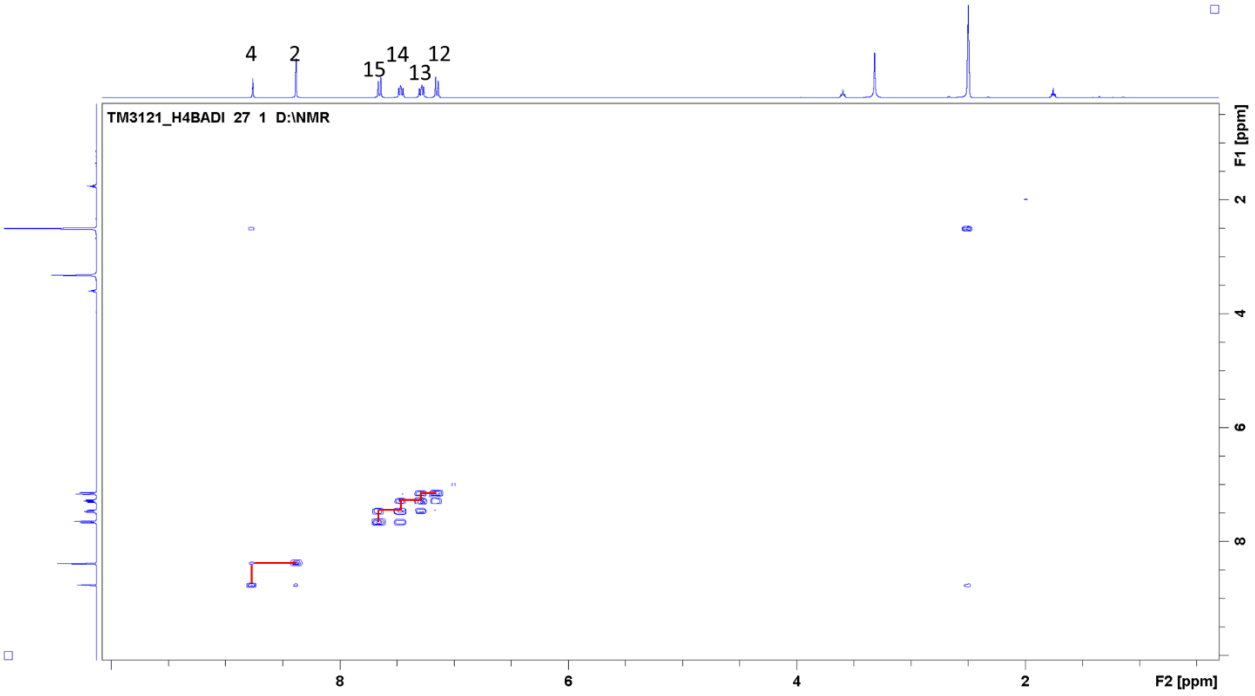

Figure S11 ^{1}H-^{1}H COSY spectrum of H_4BADI in DMSO

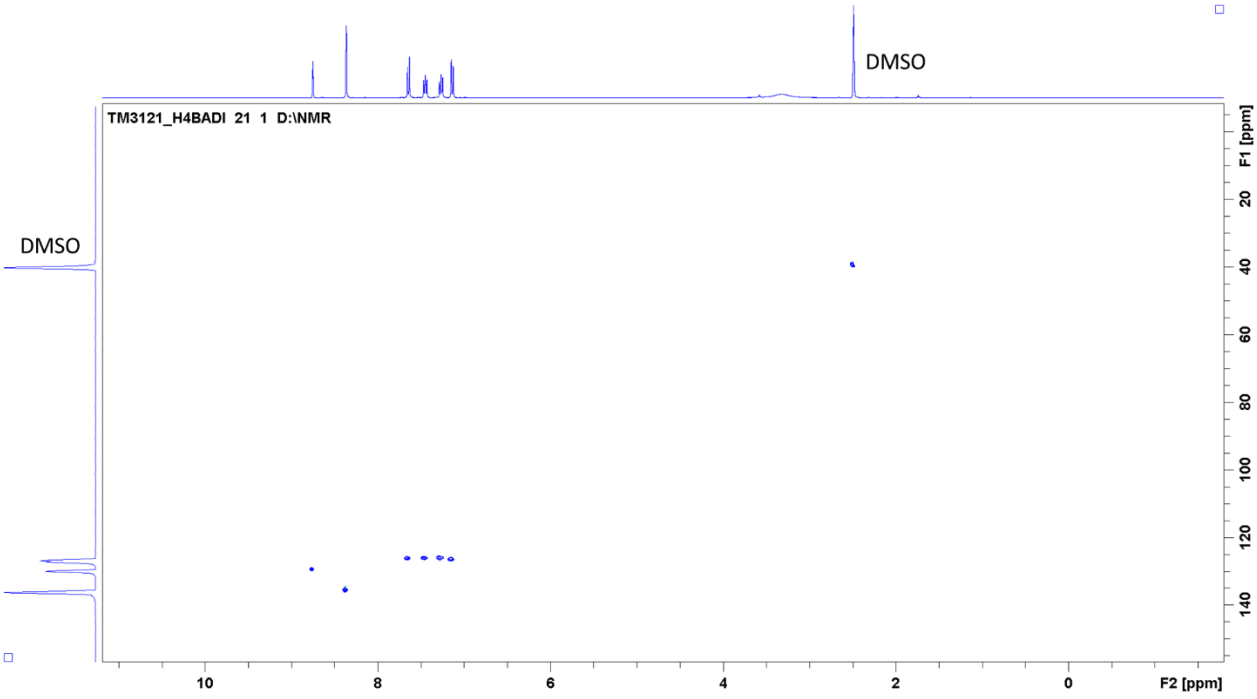

Figure S12 ^{1}H-^{13}C HSQC spectrum (full range) of H_4BADI in DMSO-d_6

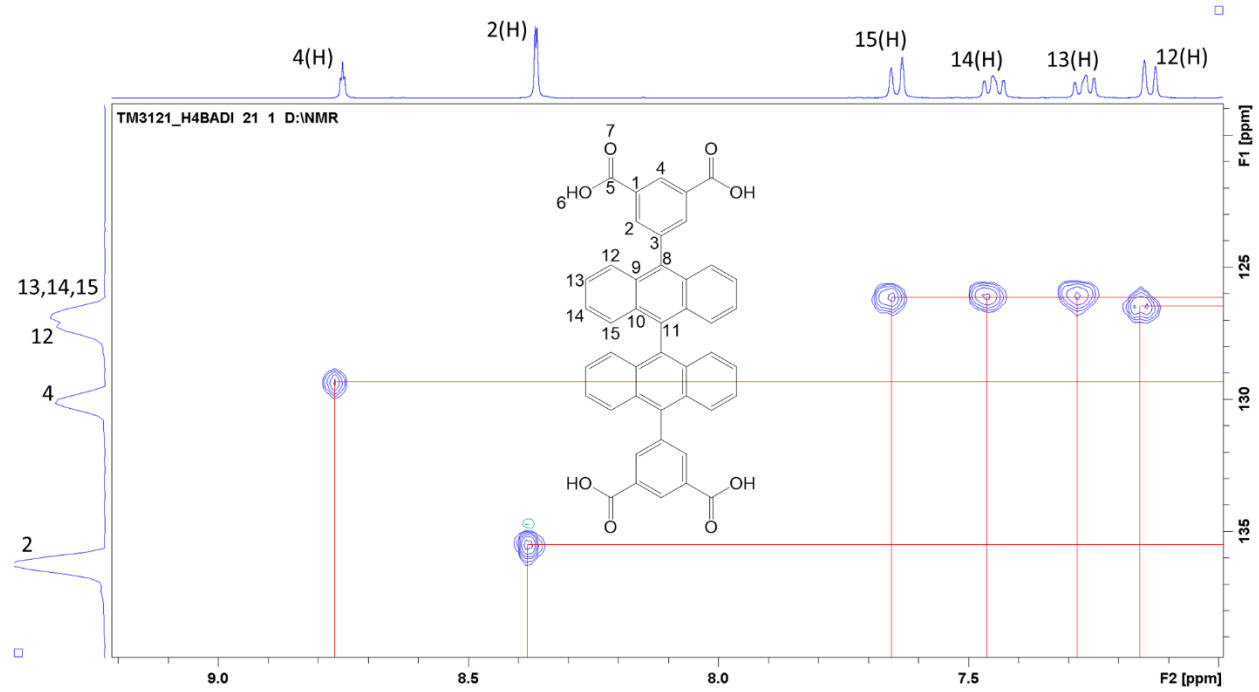

Figure S13 ^{1}H-^{13}C HSQC spectrum (zoom) of H_4BADI in DMSO-d_6

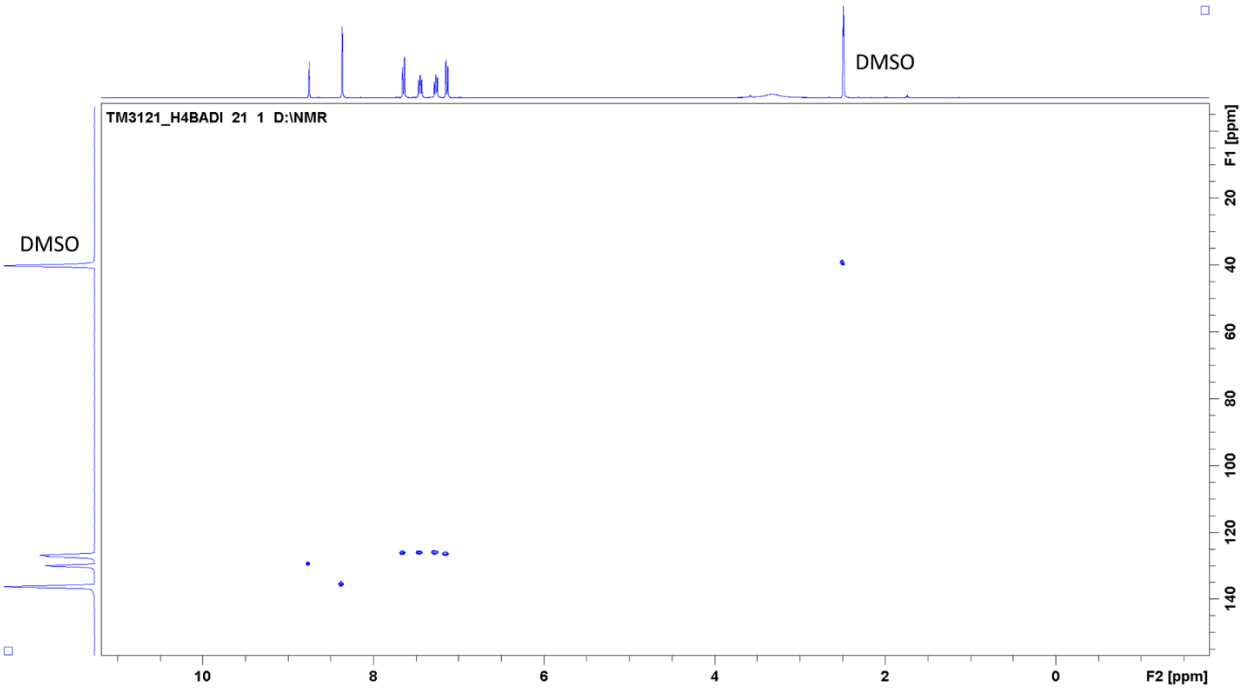

Figure S14 ^{1}H-^{13}C HMBC spectrum (full range) of H_4BADI in DMSO-d_6

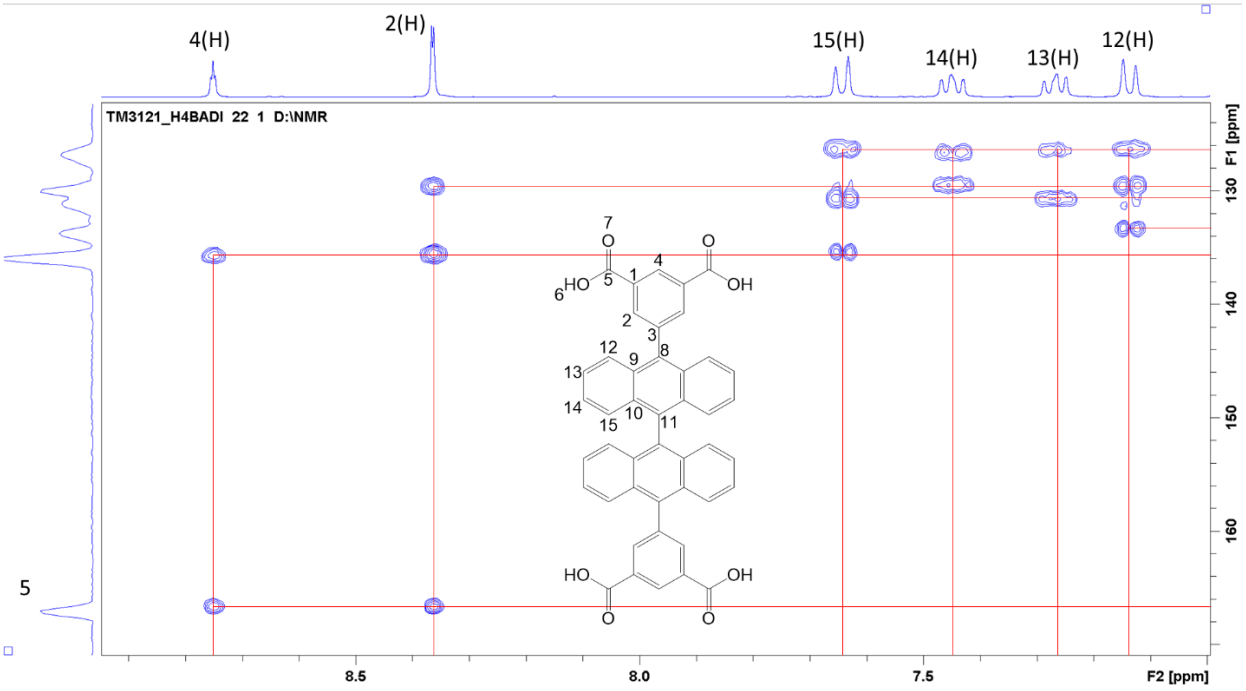

Figure S15 ^{1}H-^{13}C HMBC spectrum (zoom) of H_4BADI in DMSO-d_6

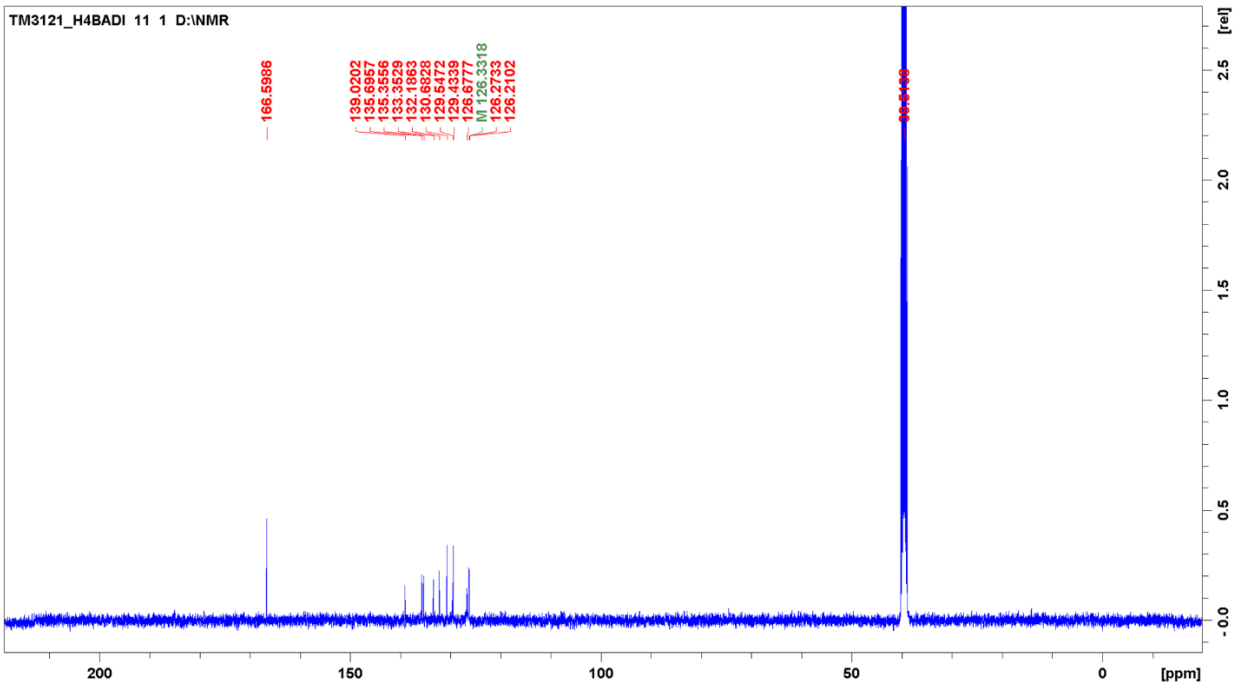

Figure S16 ^{13}C spectrum of H_4BADI in DMSO-d_6

C. Overview of MOF Synthesis

Synthetic conditions for MOF preparation were initially investigated in 1-dram vials with 1.5 mL solvent. For all screening syntheses, 5 mg ligand precursor (H_4BADI or H_4BNDI) was combined with 5 mg $Cu(NO_3)_2{\cdot}2.5H_2O$. Solvent (DMF, DMA, or DEF, 1.5 mL) was then added, followed by tetrafluoroboric acid (HBF_4, 50 – 200 µL). [Note: All synthetic attempts excluding HBF_4 from the reaction mixture resulted in observation of amorphous precipitate.] The mixture was then sonicated to dissolve, sealed with plastic screw cap, and subsequently heated at 85 °C in a digitally-controlled oven. Synthetic attempts in DMF and DEF regularly resulted in observation of Cu(0) before or concurrently with the formation of MOF, so syntheses (in oven) with DMF or DEF were eventually all conducted in uncapped vials.

Small scale reactions resulting in observation of MOF crystallites were scaled 10-fold in 20-mL scintillation vials. For these reactions, 50 mg ligand precursor (H_4BADI or H_4BNDI) was combined with 50 mg $Cu(NO_3)_2{\cdot}2.5H_2O$. Solvent (DMF or DMA, 15 mL) was then added, followed by HBF_4 (500 – 2000 µL). The reaction mixture was then sonicated to dissolve, sealed with Teflon-lined plastic screw cap, and heated at 85 °C in a digitally-controlled oven. For any of these scaled reactions the screw cap was removed at the first observation of Cu(0) formation. Eventually, all reactions involving any volume of DMF were conducted in uncapped vials. Cu(0) formation was also observed in all reactions in DMA that were heated longer than 48 h. No attempts to scale-up syntheses involving DEF were conducted.

Large-batch synthesis of Cu_2BADI-DMF was accomplished by dissolving (with sonication) 250 mg H_4BADI and 250 mg $Cu(NO_3)_2{\cdot}2.5H_2O$ in 75 mL DMF and 2.5 mL HBF_4 in a 150-mL beaker and heating (uncovered or loosely covered with a watch glass) at 85 °C in an oven for 2 days. The solid was collected via vacuum filtration, washed with fresh DMF, and dried in air (0.47 g, average of 3 trials).

ZJU-105 was isolated from all reactions between H_4BNDI and $Cu(NO_3)_2{\cdot}2.5H_2O$, regardless of solvent (DMA or DMF) and volume of HBF_4(5 – 20 µL, small scale). Syntheses in DMF resulted in crystal forms optically comparable to what was previously reported[1] (**Figure S17**), whereas syntheses in DMA resulted in crystal forms comparable to those more typically observed for **nbo**-type CuMOFs constructed from isopthalate-containing tetracarboxylates (**Figure S18**) (for example, see PCN-46 in Ref[1], and NOTT-101 and ZJNU-80 in Ref[2]). ZJU-105 could also be prepared as a fine powder in a fume hood with stirring in oil bath held at 85 °C for 48 h. To avoid co-formation of Cu(0), the reaction vial was capped with rubber septum and vent needle (20G) inserted to allow introduction of air. Heating the reaction mixture in a completely open vial resulted in evaporation of all solvent and isolation of amorphous solid.

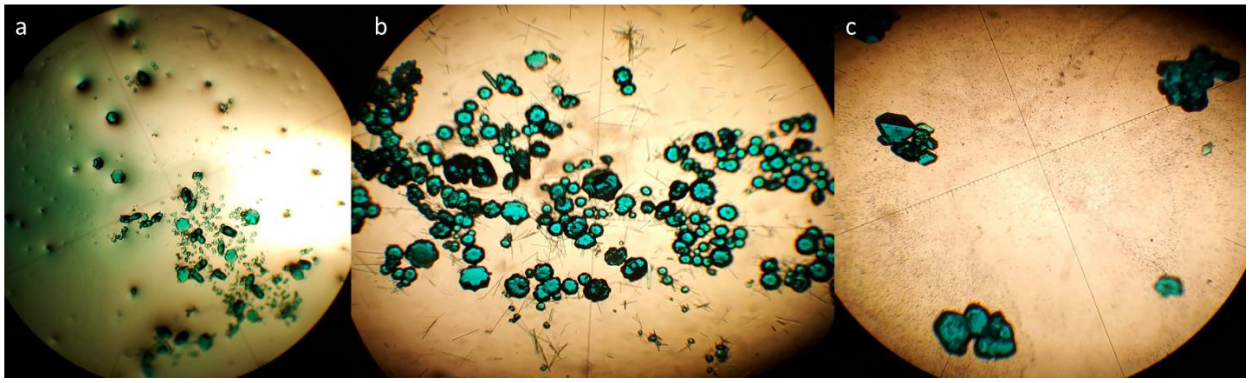

Figure S17 Optical microscopy images of ZJU-105 synthesized in DMF (85 °C): **a** 30/1, **b** 15/1, and **c** 7.5/1 v/v DMF/HBF_4

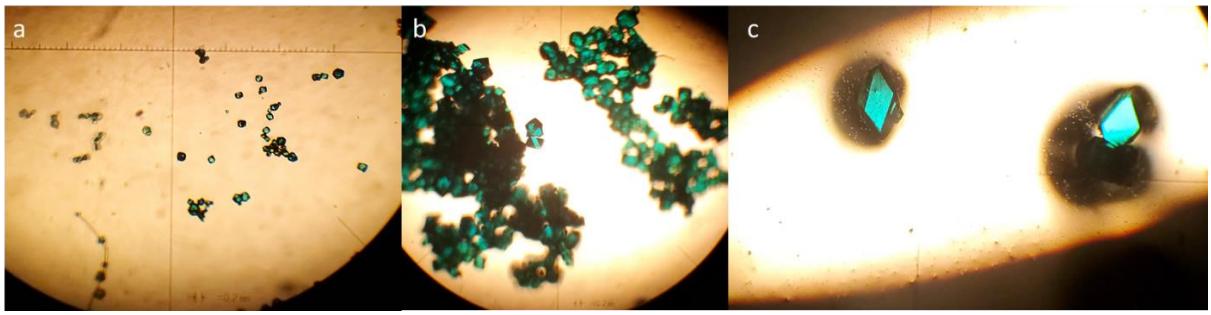

Figure S18 Optical microscopy images of ZJU-105 synthesized in DMA (85 °C): **a** 30/1, **b** 15/1, and **c** 7.5/1 v/v DMA/HBF_4

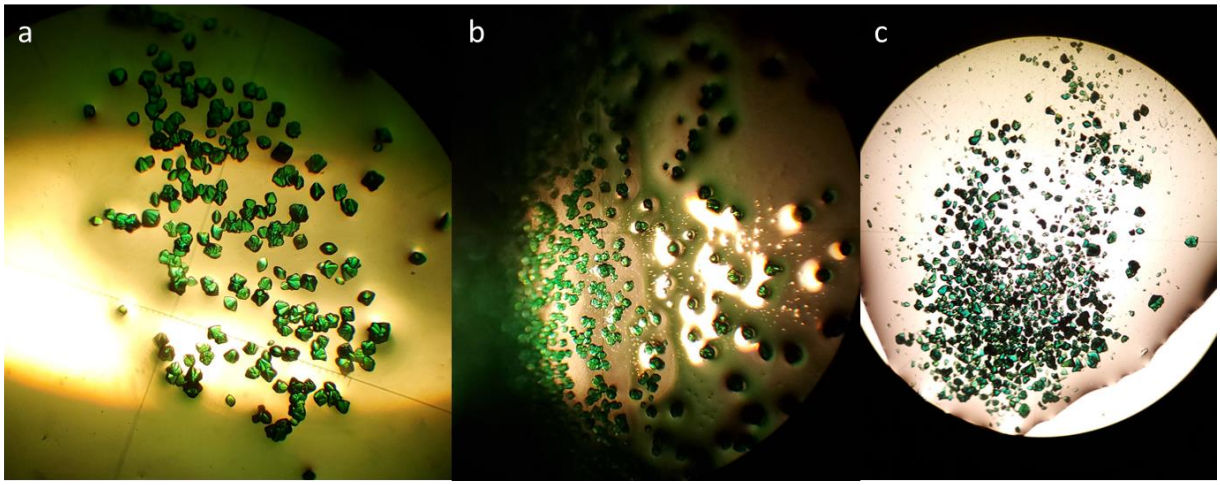

Figure S19 Optical microscopy image of Cu_2BADI-*S*: **a** DMF, **b** DMA, and **c** DEF

Alternative Synthesis of ZJU-105 (Single-crystals)

To a 20-mL scintillation vial was added H_4BNDI (0.050 g, 0.086 mmol), $Cu(NO_3)_2{\cdot}2.5H_2O$ (0.050 g, 0.21 mmol), and DMA (15 mL), followed by addition of HBF_4 (2000 µL). The vial was capped and then heated at 85 °C in an oven for 48 hours. The resultant blue crystalline material of ZJU-105 was decanted and washed with fresh DMA. Yield: 90 mg

Alternative Synthesis of ZJU-105 (Bulk powder)

To a 20-mL scintillation vial equipped with Teflon-coated magnetic stir bar was added H_4BNDI (0.050 g, 0.086 mmol), $Cu(NO_3)_2{\cdot}2.5H_2O$ (0.050 g, 0.21 mmol), and DMF (15 mL), followed by addition of HBF_4 (1000 µL). The vial was sealed with rubber septum and a vent needle (20G) added. The reaction was heated at 85 °C in an oil bath with constant stirring for 48 hours. The resultant blue-green crystalline material of ZJU-105 was decanted and washed with fresh DMF. Yield: 87 mg

Addressing Cu(0) Formation

One of the significant challenges in the preparation of novel Cu-MOFs is the prevention or remediation of Cu(0) formation during synthesis. Owing to the presence of redox-active ligands[3-6] and/or in situ formation of reducing agents from solvent decomposition[7, 8], attempted solvothermal syntheses of Cu-MOF can often result in precipitation of Cu(0). Generally, once copper metal is observed, the MOF chemist scraps the synthesis and attempts to tune reaction conditions by modifying the quantity of acid added to the reaction mixture, time of reaction, or other parameters. Alternatively, density gradients may sometimes be used to separate the Cu(0) from the desired MOF. These methods can be exceptionally tedious and time-consuming. Previous work from Jiang, et al[9] demonstrated that the continued introduction of air into a stirred MOF reaction involving redox-active ligand and Cu(II) can prevent the formation of elemental copper; however, for applications requiring larger particle sizes or for MOFs that cannot be prepared with stirring, the elimination of Cu(0) from isolated MOF product remains a challenge. To this end, we explored additional methods and modifications of those presented by Jiang, et al for remediation of Cu(0) formation during MOF synthesis. Through our investigations we have identified two alternatives to the strategies mentioned above.

Firstly, while observation of Cu(0) in a vial containing MOF is typically perceived as the "kiss of death" for the sample, we found that the Cu(0) present in many of our reaction vials containing MOF crystals can be oxidized through simply leaving the vials uncapped under laboratory conditions. Encouraged by this observation, we questioned if the oxygenation of the solution during the reaction could serve to oxidize any Cu(0) formed. We explored three variations of this experiment: (1) bubbling air into the reaction solutions prior to heating, (2) increasing the headspace above solutions in the vials, and (3) open-vial reactions. Through our studies, we found that oxygenating the solvent prior to synthesis and increasing the headspace (replacing 20-mL vial with 50-mL vial while keeping all other synthetic conditions the same) were both insufficient to prevent the formation of Cu(0).

Comparable to previous reports[9], we found that for reactions that are prone to forming Cu(0) in sealed reactions, continuous exposure to air prevented Cu(0) formation. In particular, we found that the preparation of **1**-DMF and -DEF in a sealed vial in an oven always resulted in isolation of Cu(0) in addition to crystalline MOF. Unlike what was reported by Jiang, et al[9], we found that stirring the reaction solutions in open vials was unnecessary; simply leaving the vial unsealed during synthesis was adequate. In the Jiang, et. al. report, the stirring was necessary because a solid MOF film forms at the reaction/air interface, reducing oxygen permeation to the bulk reaction mixture where the reaction was taking place. For the MOFs presented in this report, no solid film forms to impede oxygen permeation. Similarly, the preparation of bulk ZJU-105 powder in a sealed vial with stirring also resulted in formation of both Cu(0) and the desired MOF. Conducting the stirred-synthesis of ZJU-105 in an open vial was unsuccessful, owing to the complete evaporation of solvent during the reaction process. To minimize the loss of solvent, we reduced the opening aperture by sealing the vial with rubber septum and introducing a vent needle (20G) to allow for the introduction of air. This method effectively produces ZJU-105 as a microcrystalline powder while completely eliminating the co-isolation of Cu(0).

Observation of Cu(0) was uncommon in the preparation of **1**-DMA, except when the reaction mixture was heated for greater than 48 h. In such cases, the Cu(0) could be oxidized by storing the sample uncapped in its mother liquor under normal laboratory conditions for several days to weeks, depending on the amount of Cu(0) present. Heating the sample (uncapped) at 85 °C accelerated the rate of Cu(0) oxidation.

D. Single-Crystal X-ray Experimental

1-DMA X-ray Experiment

A blue prism (0.04 x 0.07 x 0.09 mm^3) was centered on the goniometer of a Rigaku Oxford Diffraction Synergy-S diffractometer equipped with a HyPix6000HE detector and operating with CuKα radiation. The data collection routine, unit cell refinement, and data processing were carried out with the program CrysAlisPro.[10] The Laue symmetry and systematic absences were consistent with the monoclinic space group $P2_1/n$. The structure was solved using SHELXT[11] and refined using SHELXL[12] via Olex2.[13] During the preliminary refinements, there was evidence of three disordered DMA molecules in the asymmetric unit; effort to model this disorder was unsuccessfully, presumably due to significant dynamic disorder with the structure cavities. Therefore, the solvent mask feature of OLEX2 was used. a total of 139.5 e^- (3 DMA molecules = 144 e^-) was subtracted from a void space of 499 $Å^3$ per asymmetric unit (558 e^- and 1996 $Å^3$ per unit cell). The final refinement model involved anisotropic displacement parameters for non-hydrogen atoms and a riding model for all hydrogen atoms.

1-DMF X-ray Experiment

An irregular shaped crystal (0.11 x 0.19 x 0.24 mm^3) was cut from a blue prism and centered on the goniometer of a Rigaku Oxford Diffraction Synergy-S diffractometer equipped with a HyPix6000HE detector and operating with MoKα radiation. The data collection routine, unit cell refinement, and data processing were carried out with the program CrysAlisPro.[10] The Laue symmetry and systematic absences were consistent with the orthorhombic space group *Cccm* (#63). However, in this space group, there were systematically weak reflection suggesting a superlattice and the preliminary structure model showed significant disorder with unreasonable steric interactions. Upon more careful analysis of the diffraction data, a monoclinic nonmerohedral twin was identified (twin law 180° rotation about [001]) that accounted for the majority of the systematically weak reflection. During structure refinement on the HLKF 5 twin data, the twin ratios refined to approximately 50/50 (0.516(2) and 0.484(2)) accounting for the pseudo orthorhombic symmetry.

The structure was solved in space group *P*2/*c* (#13) using SHELXT[11] and refined using SHELXL[12] via Olex2.[13] Unlike the *Cccm* model, the $BADI^{4-}$ ligand is fully ordered in *P*2/*c*. The capping ligands of the paddlewheel complex are modeled as water but are likely a combination of water and DMF based on the presence of multiple difference electron density peaks near the coordinated oxygen. Attempt to model partial DMF occupancy at this site were unsuccessful–presumably the DMF is in dynamic motion. There is also evidence of multiple disordered DMF molecules in the solvent cavities. Using the solvent mask feature of OLEX2, a total of 893 e^-, equivalent to ~22 DMF molecules (880 e^-) was subtracted from 3665 $Å^3$ total void space per unit cell, or ~5.5 DMF per asymmetric unit (223 e^-/916 Å). The final refinement model involved anisotropic displacement parameters for non-hydrogen atoms and a riding model for all hydrogen atoms.

1-DMSO X-ray Experiment

A blue plate (0.02 x 0.07 x 0.15 mm^3) was centered on the goniometer of a Rigaku Oxford Diffraction Synergy-S diffractometer equipped with a HyPix6000HE detector and operating with CuKα radiation. The data collection routine, unit cell refinement, and data processing were carried out with the program

CrysAlisPro.[10] The Laue symmetry and systematic absences were consistent with the orthorhombic space group *Cccm* (#63). However, based on the structure of **1**-DMF (CCDC 2324985), we know that this space group occurs from pseudomerohedral twinning of space group *P*2/*c*. Unfortunately, this sample exhibited both multi-crystal (i.e., nonmerohedral) and pseudomerohedral twinning. As a result, we were unable to obtain suitable quality data to refine in P2/c. Therefore, our only option was to process as the orthorhombic pseudomerohedral twin and refine as disordered in *Cccm*. The structure was solved using SHELXT[11] and refined using SHELXL[12] via Olex2.[13] The capping ligands of the paddlewheel complex are modeled as water but are likely a combination of water and DMSO. A 2-position disorder model was used for the anthracene fragments with relative occupancies constrained to 50% by symmetry. The solvent mask feature of OLEX2, was used to subtract out a total of 835 e^-, equivalent to ~20 DMSO molecules (840 e^-) from 2698 $Å^3$ total void space per unit cell, or ~1.25 DMSO per asymmetric unit. The final refinement model involved anisotropic displacement parameters for non-hydrogen atoms and a riding model for all hydrogen atoms.

Table S1 Crystal and structure refinement data for **1**-DMA, **1**-DMF, **1**-DMSO, and **2**

	1-DMA	**1**-DMF	**1**-DMSO	**2**
Empirical Formula	$C_{64}H_{67}Cu_2N_5O_{13}$	$C_{60.5}H_{60.5}Cu_2N_{5.5}O_{15.5}$	$C_{54}H_{52}Cu_2O_{15}S_5$	$C_{34}H_{39}N_4O_8Zn$
Formula Weight	1241.3	1239.72	1228.33	697.06
Temperature/K	100.00(10)	100.0(2)	99.9(3)	100.0(2)
Radiation	Cu Kα	Mo Kα	Cu Kα	Cu Kα
Wavelength	1.54184	0.71073	1.54184	1.54184
Crystal System	monoclinic	monoclinic	orthorhombic	orthorhombic
Space Group	$P2_1/n$	P2/c	Cccm	Fdd2
a/Å	10.7147(2)	19.1907(3)	10.4087(3)	38.9726(6)
b/Å	37.1847(6)	14.79129(19)	36.7583(8)	24.8157(5)
c/Å	14.7691(2)	22.8997(6)	15.4789(4)	13.8024(2)
α/°	90	90	90	90
β/°	92.982(2)	107.262(2)	90	90
γ/°	90	90	90	90
V/Å^3	5876.38(17)	6207.4(2)	5922.3(3)	13348.7(4)
Z	4	4	4	16
ρ_{calc} g/cm^3	1.403	1.327	1.378	1.387
μ/mm^{-1}	1.467	0.754	3.055	1.498
F(000)	2592.0	2576	2536.0	5840
Crystal size/mm^3	0.09 × 0.07 × 0.04	0.262 × 0.162 × 0.123	0.15 × 0.07 × 0.02	0.16 × 0.09 × 0.06
Reflections coll.	47605	29748	31846	30940
Independent refl.	11844	29748	3226	6325
R_{int} value	0.0622		0.0808	0.0485
GooF	1.048	1.076	1.077	1.048
R indices [I>2σ(I)]	R_1 = 0.0555 wR_2 = 0.1421	R_1 = 0.1000 wR_2 = 0.2859	R_1 = 0.0671 wR_2 = 0.1987	R_1 = 0.0762 wR_2 = 0.2121
R indices (all data)	R_1 = 0.0698 wR_2 = 0.1491	R_1 = 0.1418 wR_2 = 0.3179	R_1 = 0.0758 wR_2 = 0.2056	R_1 = 0.0801 wR_2 = 0.2194

E. MOF Structures

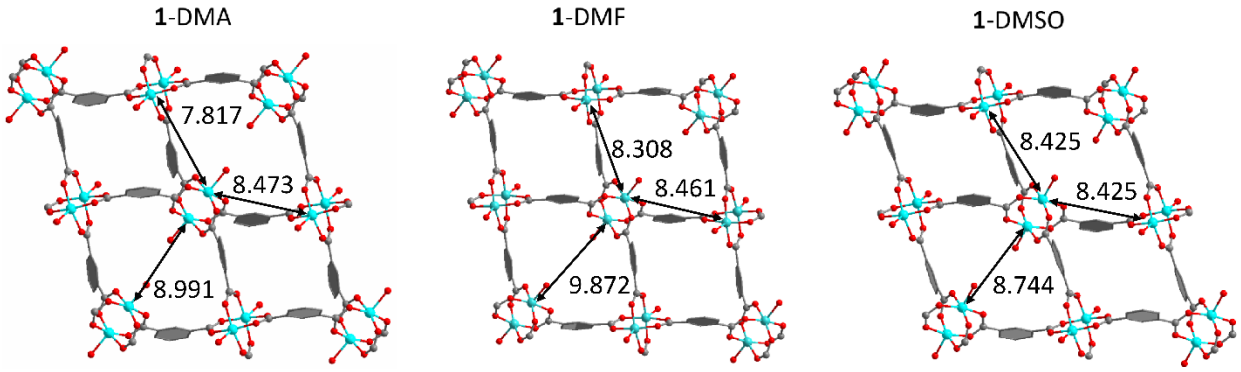

Figure S20 Metal-isophthalate layers present in **1**-*S* with nearest Cu-Cu distance measurements labeled. Metal-isophthalate layers span the third dimension through bianthracenyl moieities extending from the 5-position of each isophthalate group

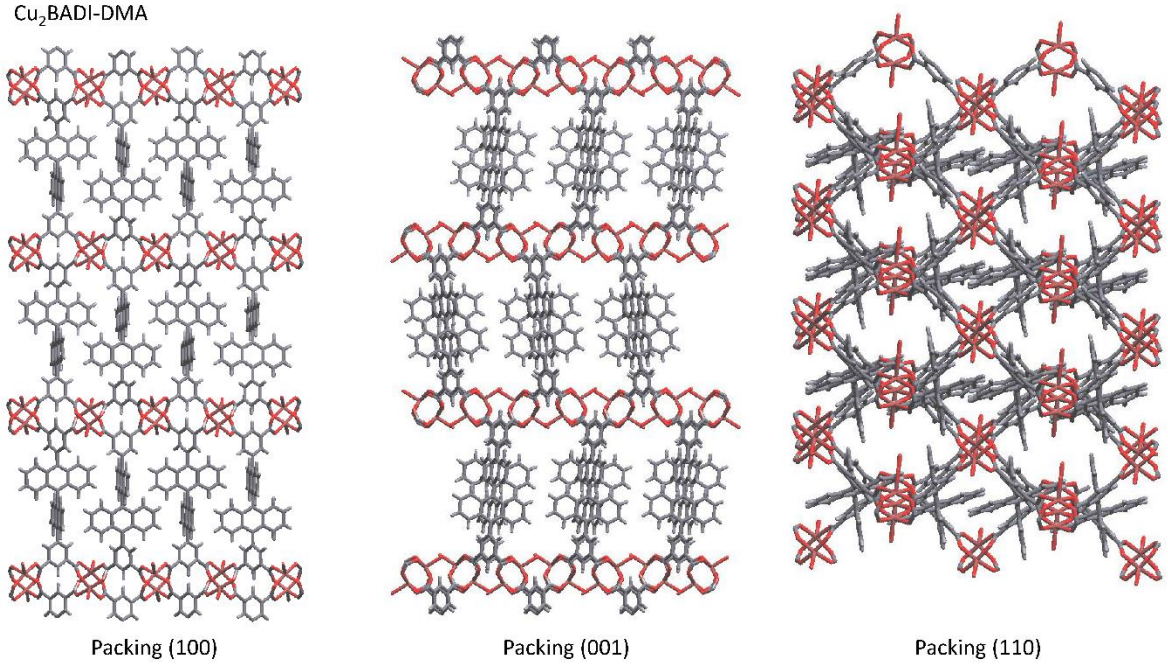

Figure S21 Crystal packing in **1**-DMA

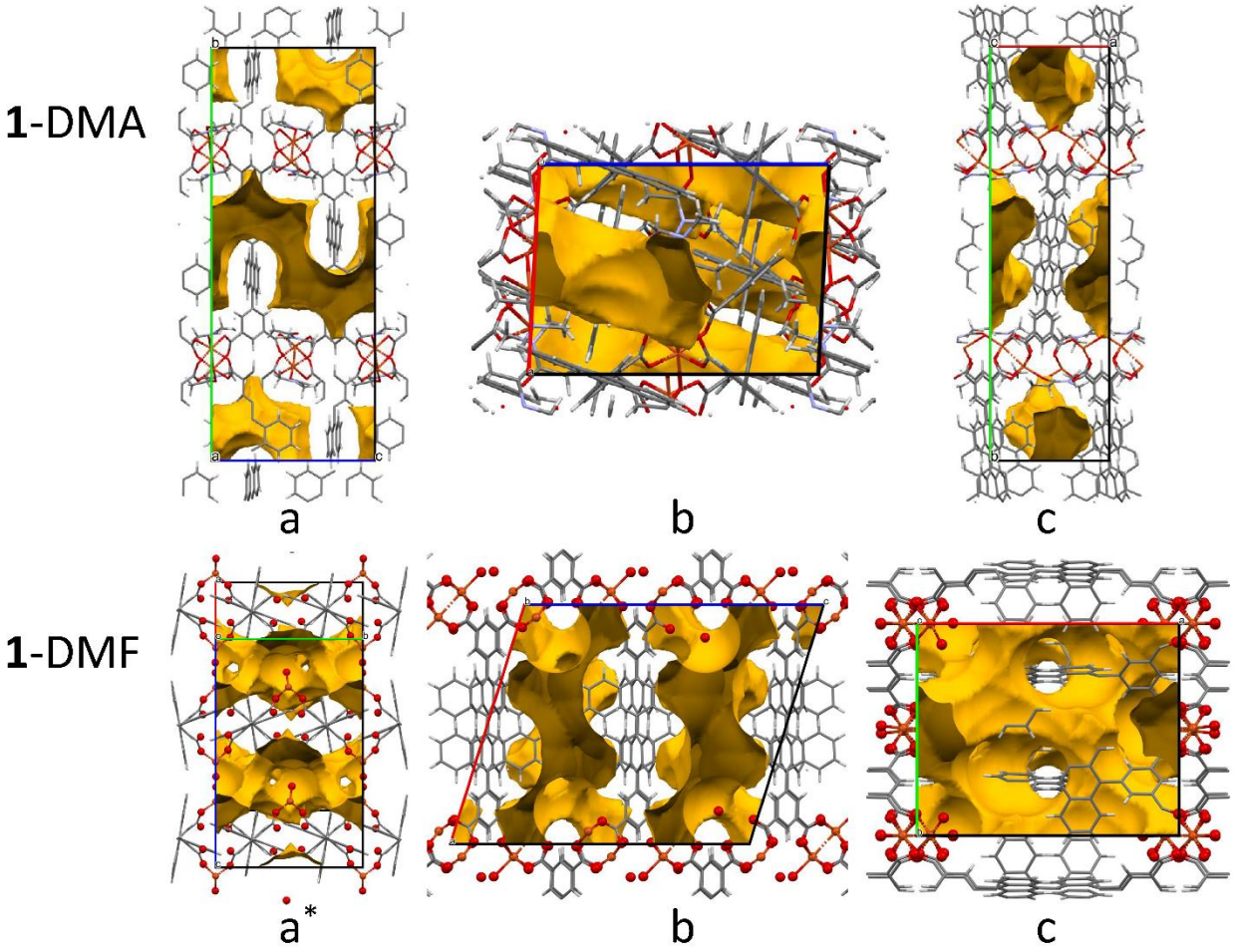

Figure S22 Solvent-accessible voids in **1**-DMA and -DMF as calculated using the *Mercury* program with spherical probe with 1.2 Å radius.[14]

Table S2 Unit cell parameters of **1**-*S*

Crystal	*a* (Å)	*b* (Å)	*c* (Å)	α (°)	β (°)	γ (°)	V (Å^3)
1-DMA	10.7147	37.1847	14.7691	90	92.982	90	5876.38
1-DMF	19.1907	14.79129	22.8997	90	107.262	90	6207.42
1-DMF (ortho)*	11.3494	36.6729	14.7750	90	90	90	6149.58
1-DMSO	10.4087	36.7583	15.4789	90	90	90	5922.32

*__1__-DMF(ortho) = __1__-DMF structure solved and refined in the orthorhombic space group *Cccm*

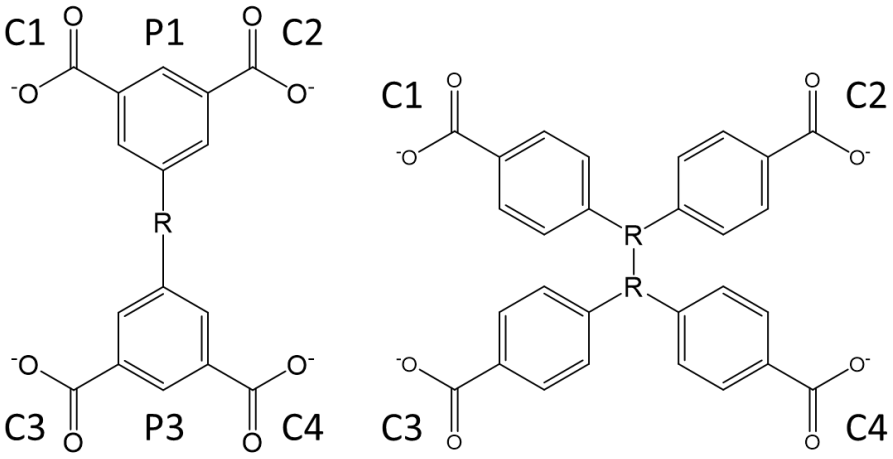

Figure S23 Labeling system used for identifying dihedral angles between planes prepared from O-C-O atoms in carboxylates (C1 – C4) and carbon atoms in phenyl rings (P1 and P3) in diisophthalate (left) and tetrabenzoate (right) ligands

Table S3 Dihedral angles between planes generated from carboxylates and phenyl (isophthalate) rings in several MOFs composed of dicopper paddlewheel and diisophthalate-containing ligands. Previously-reported MOFs are grouped by net topology. Labeling system presented in Figure S23

MOF	Space Group	Dihedral Angles between planes (degrees)														
		P1 P3	**P1 C1**	**P1 C2**	**P1 C3**	**P1 C4**	**P3 C1**	**P3 C2**	**P3 C3**	**P3 C4**	**C1 C2**	**C1 C3**	**C1 C4**	**C2 C3**	**C2 C4**	**C3 C4**
1-DMA	$P2_1/n$	80	38	26	88	86	79	87	32	32	54	87	54	66	86	59
1-DMF	$P2/c$	82	30	24	88	82	85	87	29	33	48	89	59	68	83	56
1-DMF (ortho)	*Cccm*	82	29	29	86	86	86	86	29	29	52	87	64	64	87	52
1-DMSO	*Cccm*	70	33	33	87	87	87	87	33	33	57	87	66	66	87	57
Nbo/fof* MOFs																
ZJU-105[1]	*R*-3*m*	0	5	5	5	5	5	5	5	5	6	6	0	0	6	6
NOTT-102[15]	*R*-3*m*	0	7	7	7	7	7	7	7	7	8	8	0	0	8	8
Cu_2ADEDA[16]	*R*-3*m*	0	5	5	5	5	5	5	5	5	7	7	0	0	7	7
PCN-14[17]	*R*-3*c*	0	6	8	8	6	6	8	8	6	12	12	0	0	12	12
ssb/stx* MOF																
NOTT-109[15]	*I*4/*mmm*	18	18	18	34	34	34	34	18	18	22	46	52	52	46	22

*Topologies presented as net formed from treatment of the ligand as four-connected node and two three-connected nodes [ie, (net from 4-c ligand)/(net from $(3\text{-c})^2$ ligand)]

Table S4 Dihedral angles between planes generated from carboxylates in several MOFs composed of dicopper paddlewheel and tetrabenzoate-containing ligands and **1**-*S* (reproduced from Table S3). All MOFs reported in Table S4 have **pts**-net topology except Cu_2TCPPDA (*Imma*), which is **lvt**-net topology. Labeling system presented in Figure S23

MOF	Space Group	Dihedral Angles between Planes (degrees)					
		C1 C2	**C1 C3**	**C1 C4**	**C2 C3**	**C2 C4**	**C3 C4**
PCN-39m[18]	*C*2/*c*	36	52	78	78	52	51
PCN-39t[18]	*P*-1	44	50	80	86	51	50
PCN-38[18,†]	*P*-1	49 (52)	46 (44)	81 (80)	81 (83)	61 (70)	53 (36)
Cu_2TCPPDA[19]	*Cccm*	66	86	58	58	86	66
Cu_2TCPPDA[19]	*Imma**	63	63	0	0	63	63
1-DMA	$P2_1/n$	60	87	54	67	87	54
1-DMF	*P*2/*c*	53	88	65	65	88	53
1-DMF (ortho)	*Cccm*	52	88	64	64	88	52
1-DMSO	*Cccm*	57	87	66	66	87	57

[†]PCN-38 contains two ligands in the asymmetric unit. Angles are reported between groups within one ligand. Angles for the second ligand are reported in parentheses.

*Cu_2TCPPDA (*Imma*) adopts an **lvt**-net topology, though previously reported as **nbo**

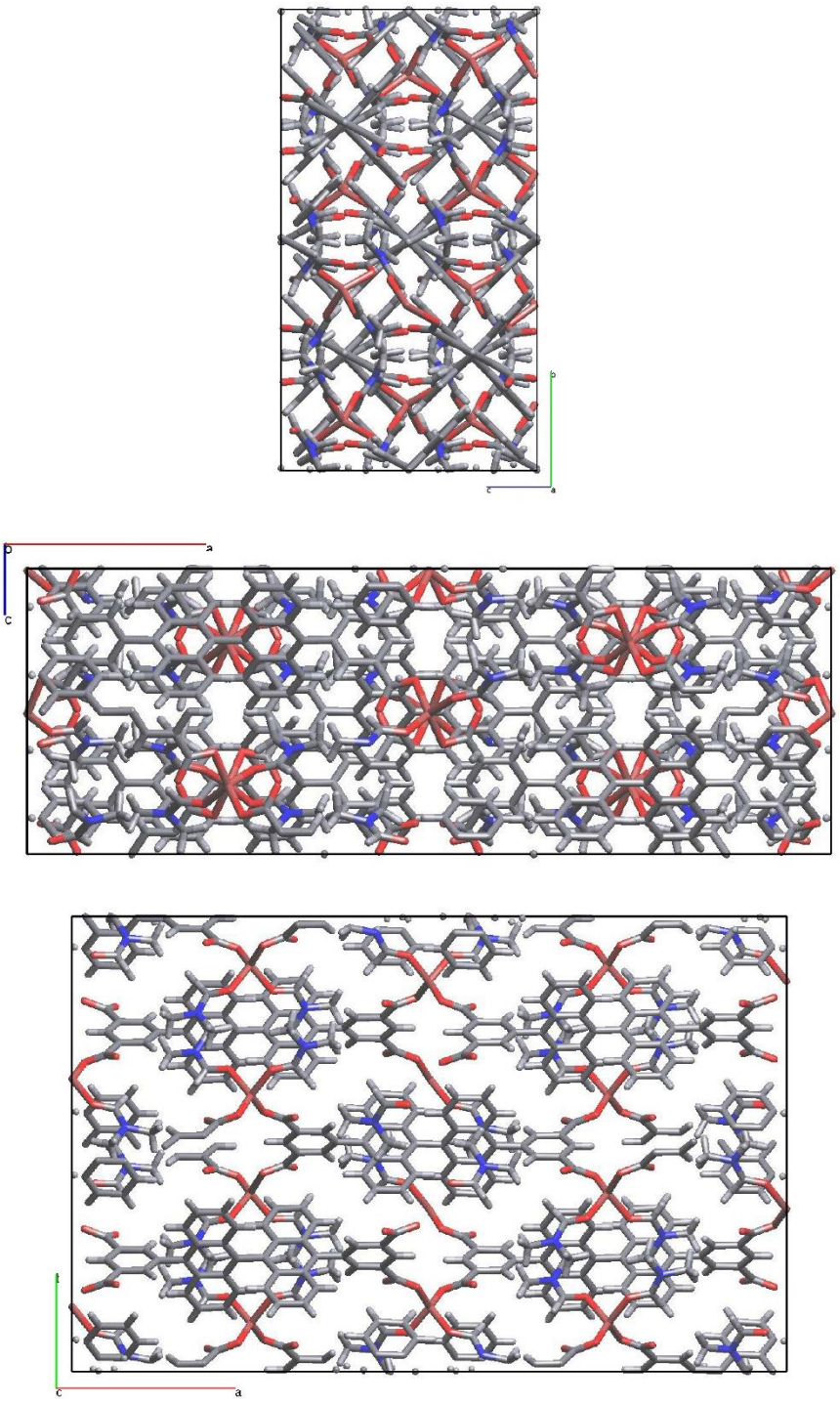

Figure S24 Crystal packing in **2** viewed down the *a*- (top), *b*- (middle), and *c*-axes (bottom). Noncoordinated solvent molecules are removed for clarity. Rose = zinc, red = oxygen, blue = nitrogen, dark gray = carbon, light gray = hydrogen.

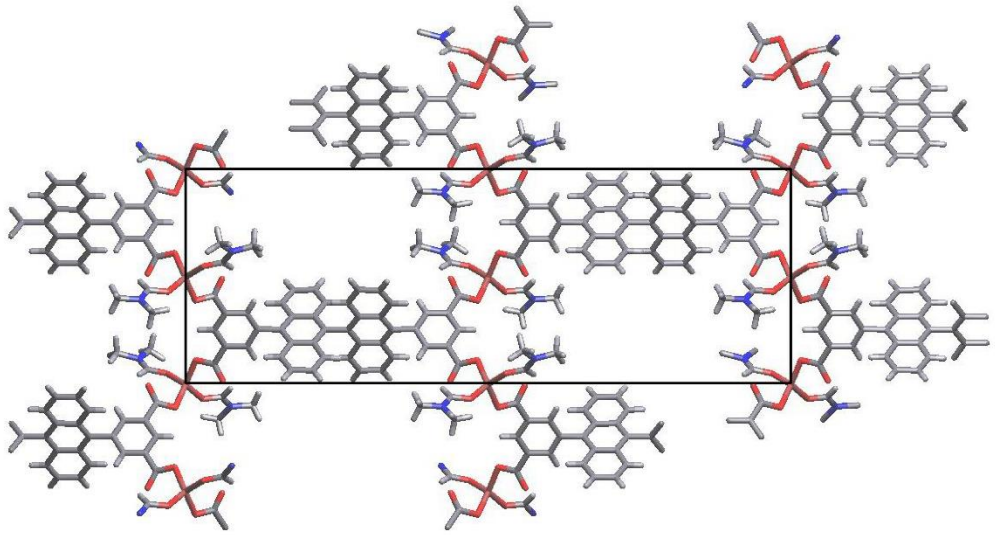

Figure S25 Single $Zn_2BADI(DMF)_2$ 2-D layer in **2** viewed down the *b*-axis.

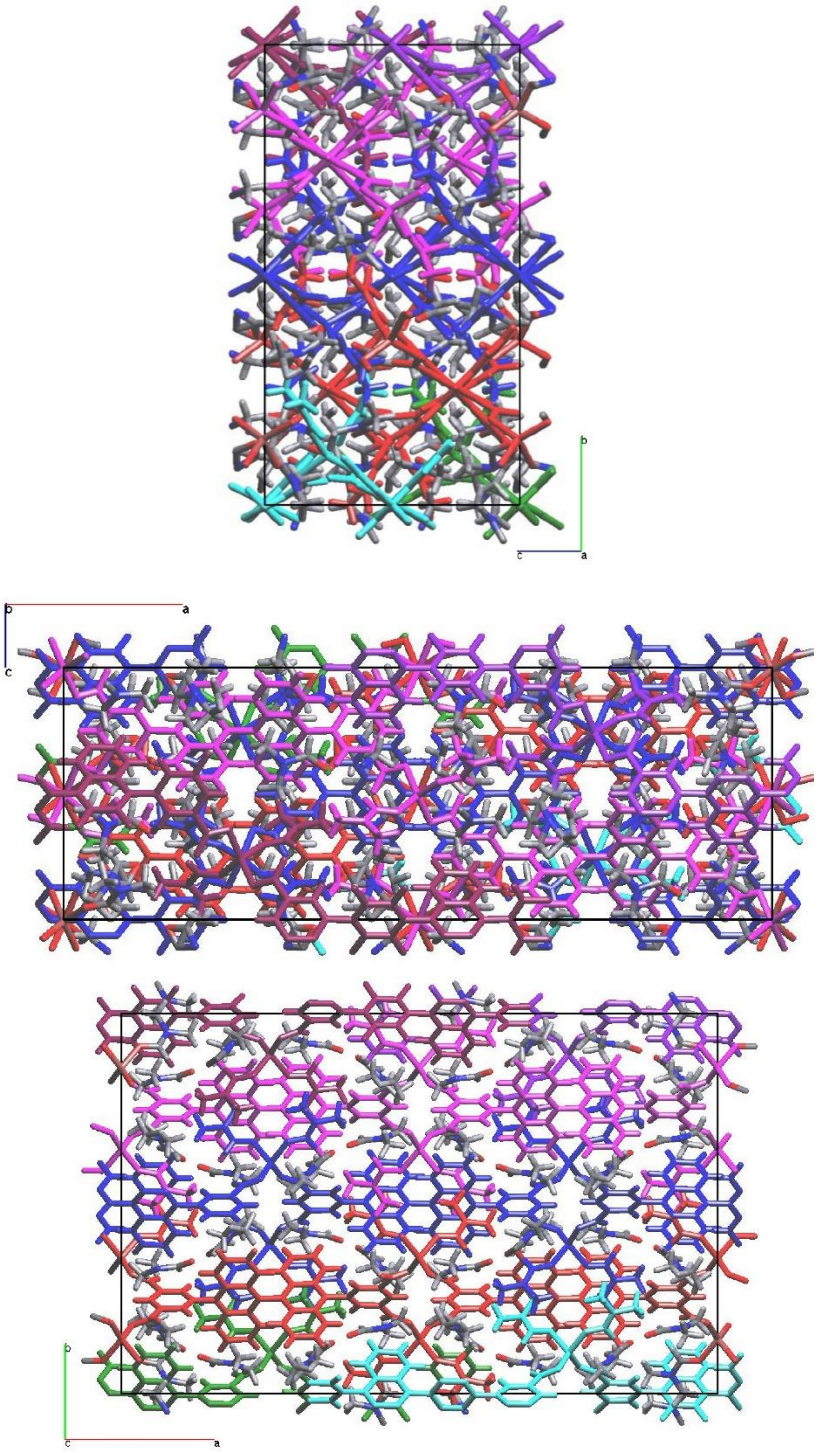

Figure S26 Crystal packing in Zn_2BADI viewed down the *a*- (top), *b*- (middle), and *c*-axes. Separate 2-D layers are represented as individual colors to highlight positions of free-solvent molecules. Dark gray = carbon, blue(individual atoms) = nitrogen, red(individual atoms) = oxygen, light gray = hydrogen.

F. PXRD Data

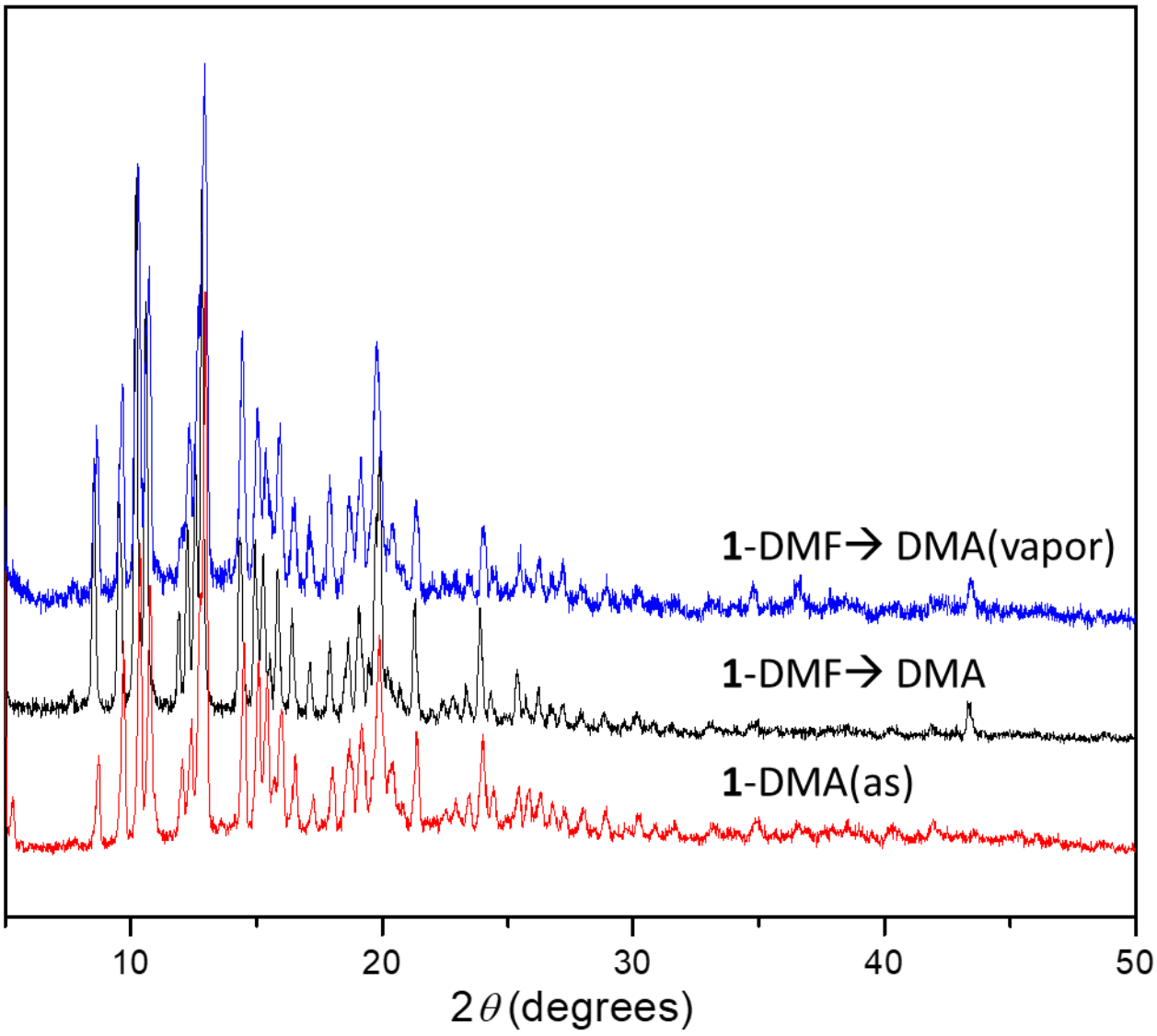

Figure S27 PXRD patterns of **1**-DMF after soaking in DMA compared to **1**-DMA(as) (**1**-S_1→S_2 = **1**-S_1 soaked in S_2 for 18 h at 85 °C)

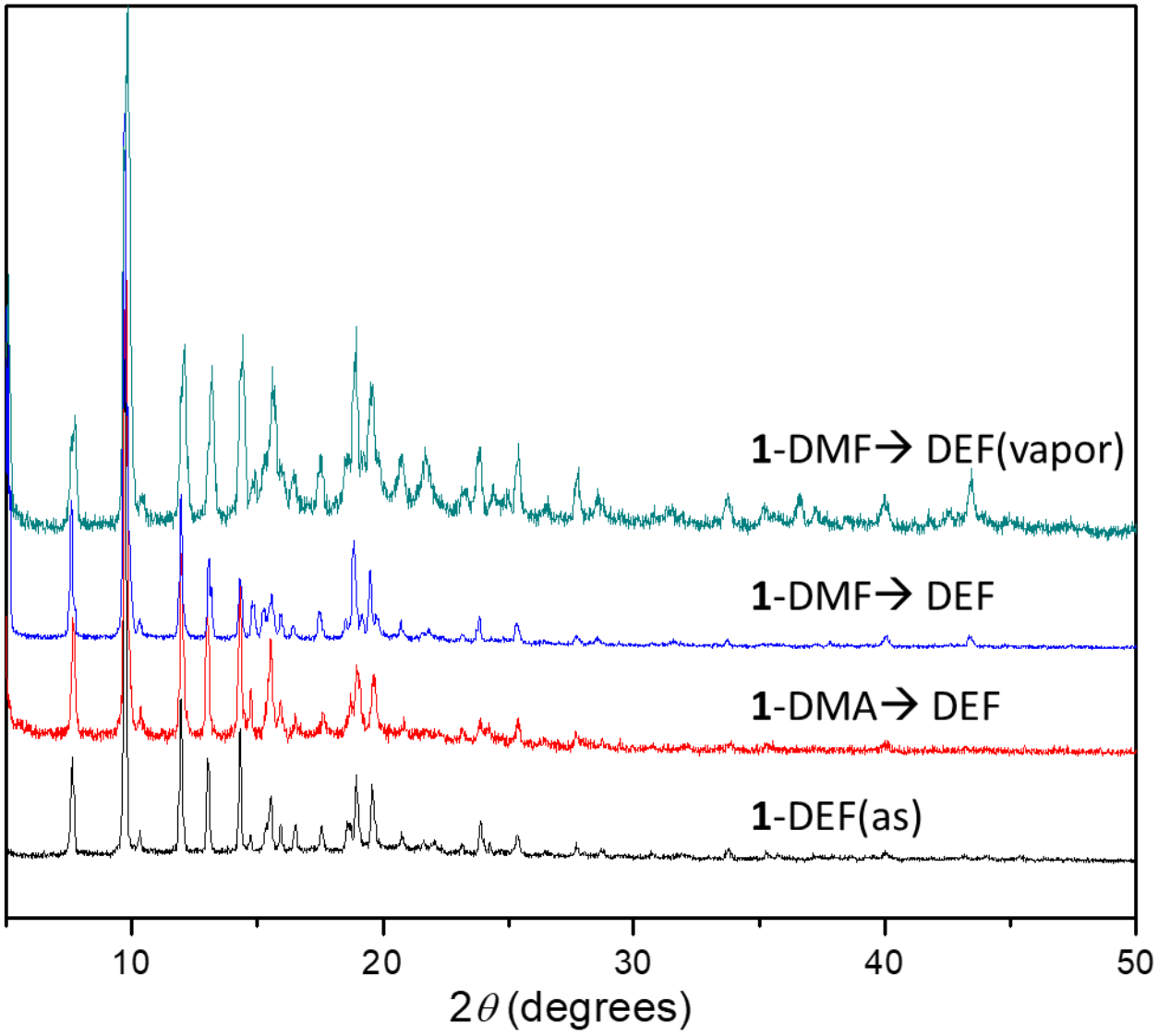

Figure S28 PXRD patterns of **1**-*S* after soaking in DEF compared to **1**-DMA(as) (**1**-S_1→S_2 = **1**-S_1 soaked in S_2 for 18 h at 85 °C), and **1**-DMF exposed to DEF vapor at 85 °C for 18 h

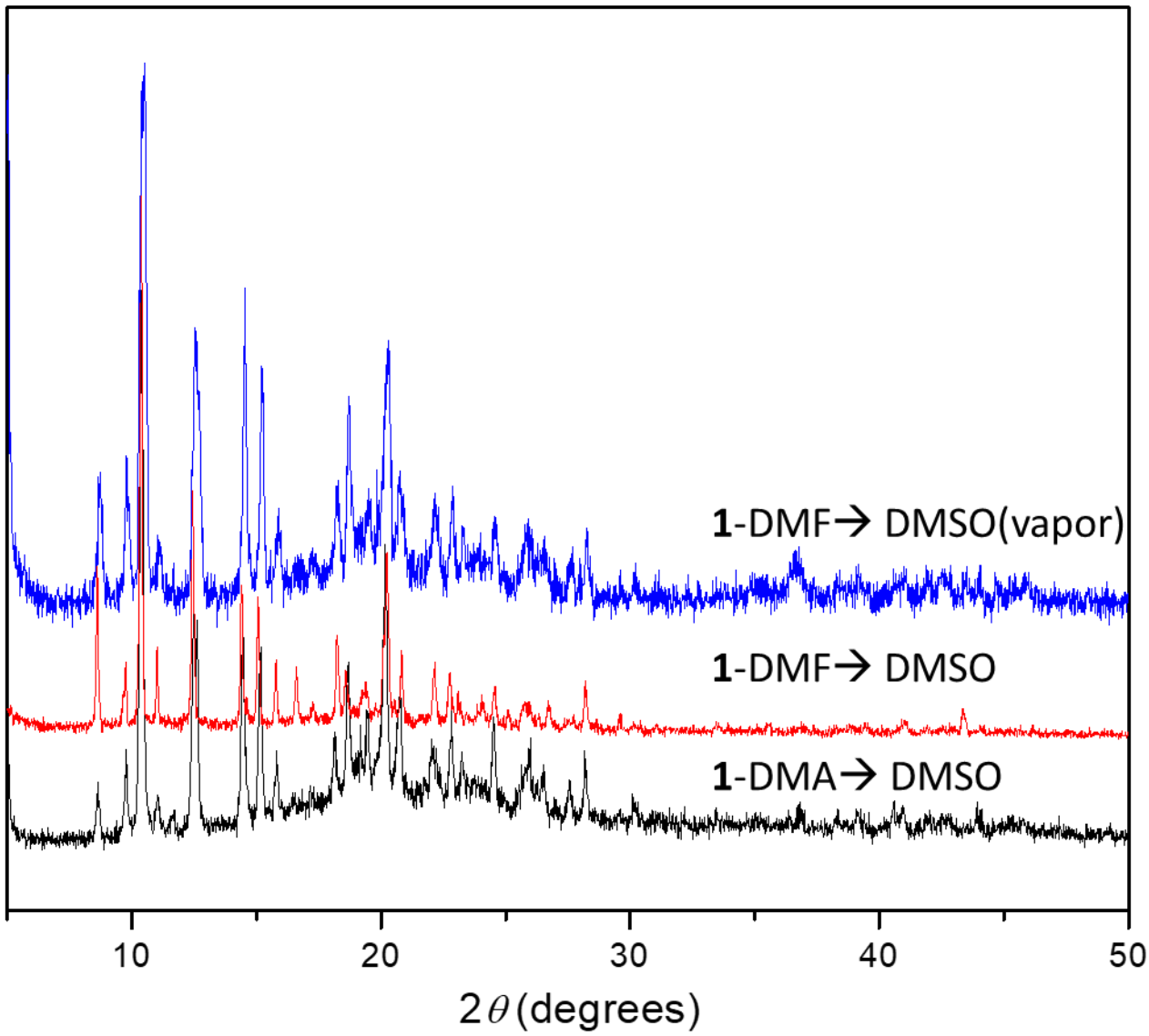

Figure S29 PXRD patterns of **1**-*S* after soaking in DMSO (**1**-S_1→S_2 = **1**-S_1 soaked in S_2 for 18 h at 85 °C), and **1**-DMF exposed to DMSO vapor at 85 °C for 18 h

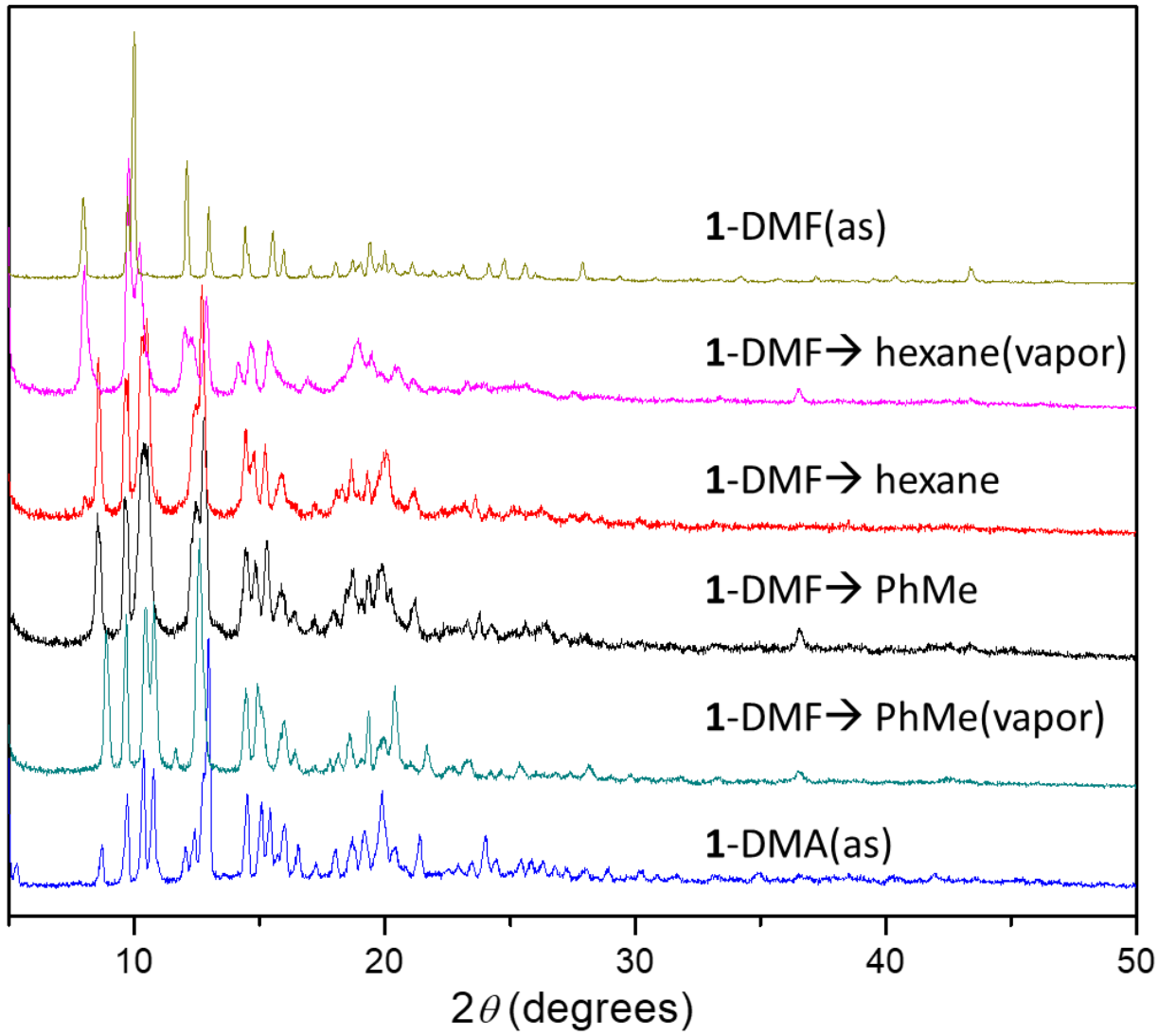

Figure S30 PXRD patterns of **1**-DMF after soaking in nonpolar solvent, or exposed to nonpolar solvent vapor compared to **1**-DMA(as) and **1**-DMF(as). Samples exposed to toluene (PhMe) were heated at 85 °C, while those exposed to hexane were kept at ambient temperature.

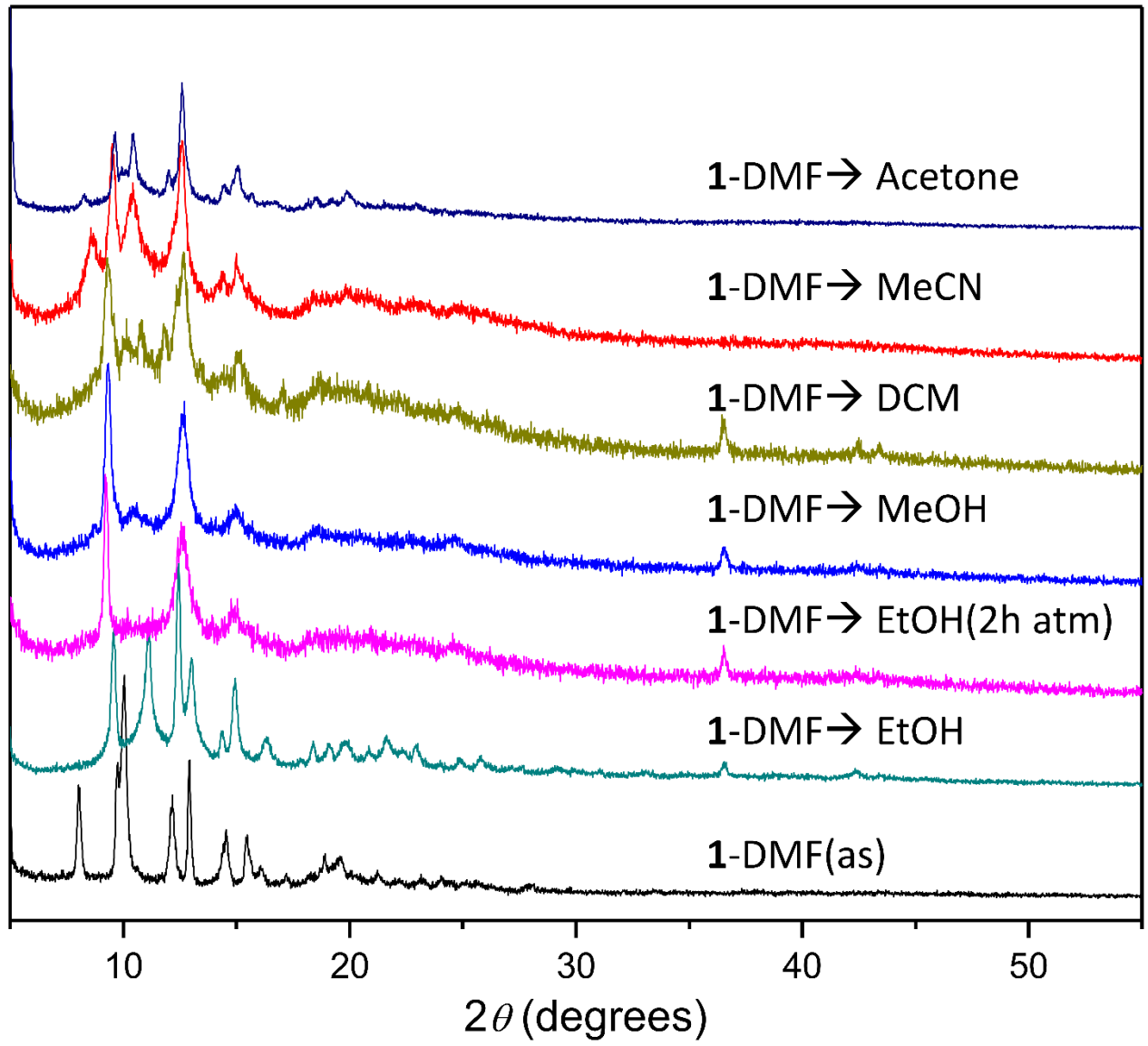

Figure S31 PXRD patterns of **1**-*S* after soaking in volatile, polar solvent (**1**-S_1→S_2 = **1**-S_1 soaked in S_2 for 18 h at ambient temperature). "**1**-DMF→ EtOH(2h atm)" = **1**-DMF→ EtOH after 2 hours exposure to atmospheric conditions in the laboratory.

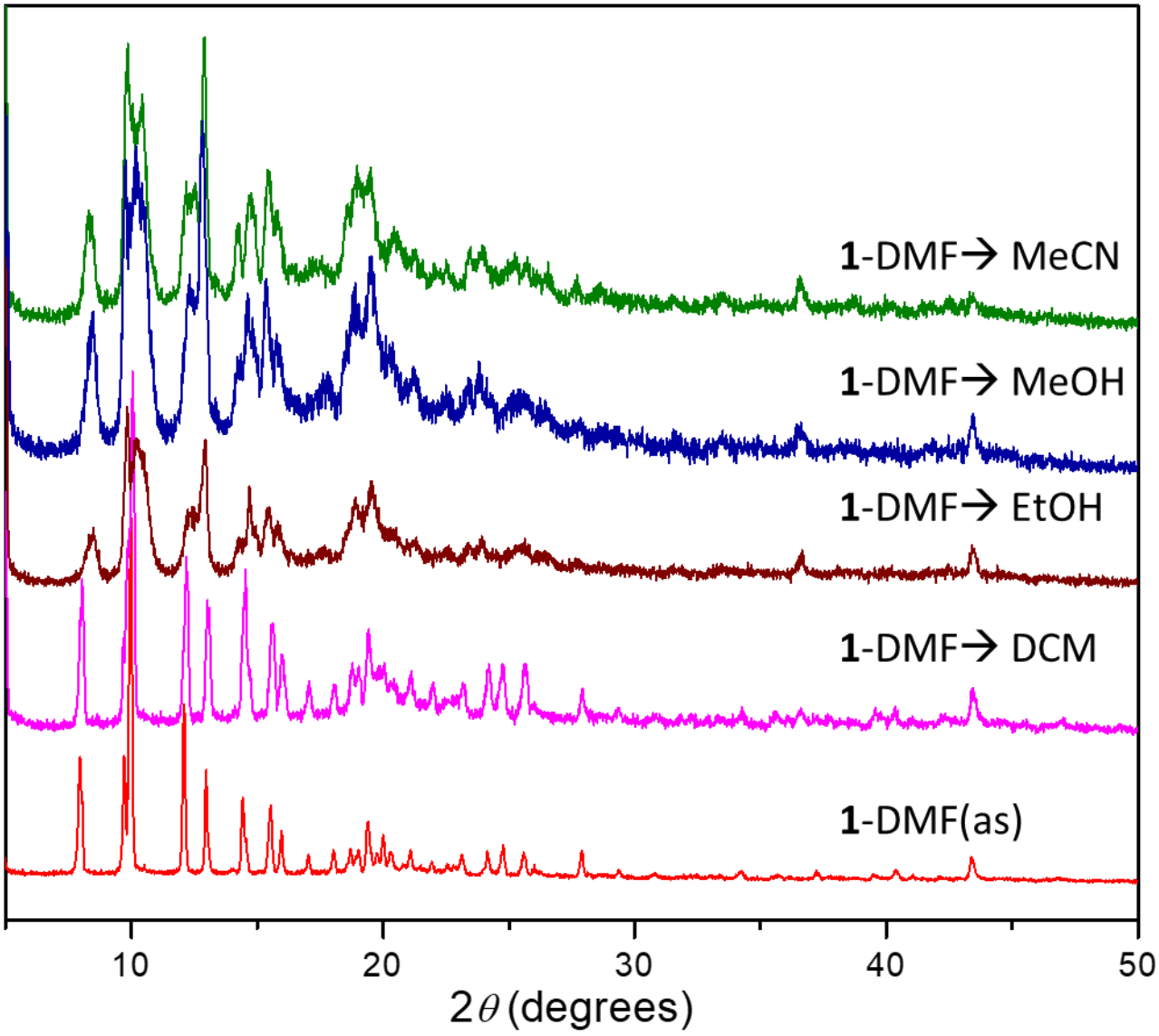

Figure S32 PXRD patterns of **1**-*S* after exposure to volatile, polar solvent vapor (**1**-S_1→S_2 = **1**-S_1 exposed to S_2 vapor for 18 h at ambient temperature)

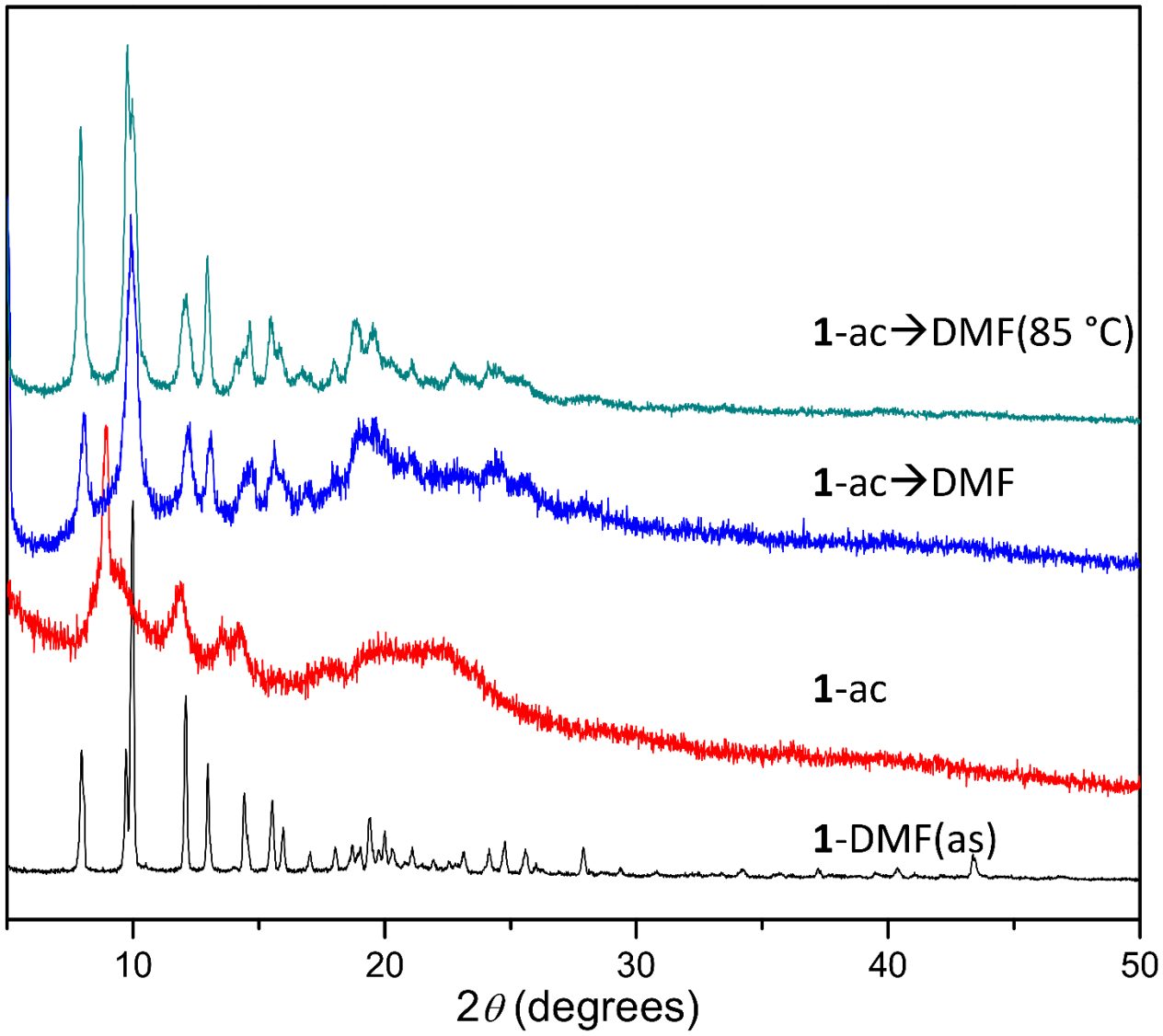

Figure S33 PXRD patterns of **1**-DMF after activation (**1**-ac), and the activated sample soaked in DMF at room temperature for 18 h (**1**-ac→DMF) and heated at 85 °C in DMF for 24 h (**1**-ac→DMF(85 °C)).

G. Thermogravimetric Analysis Data

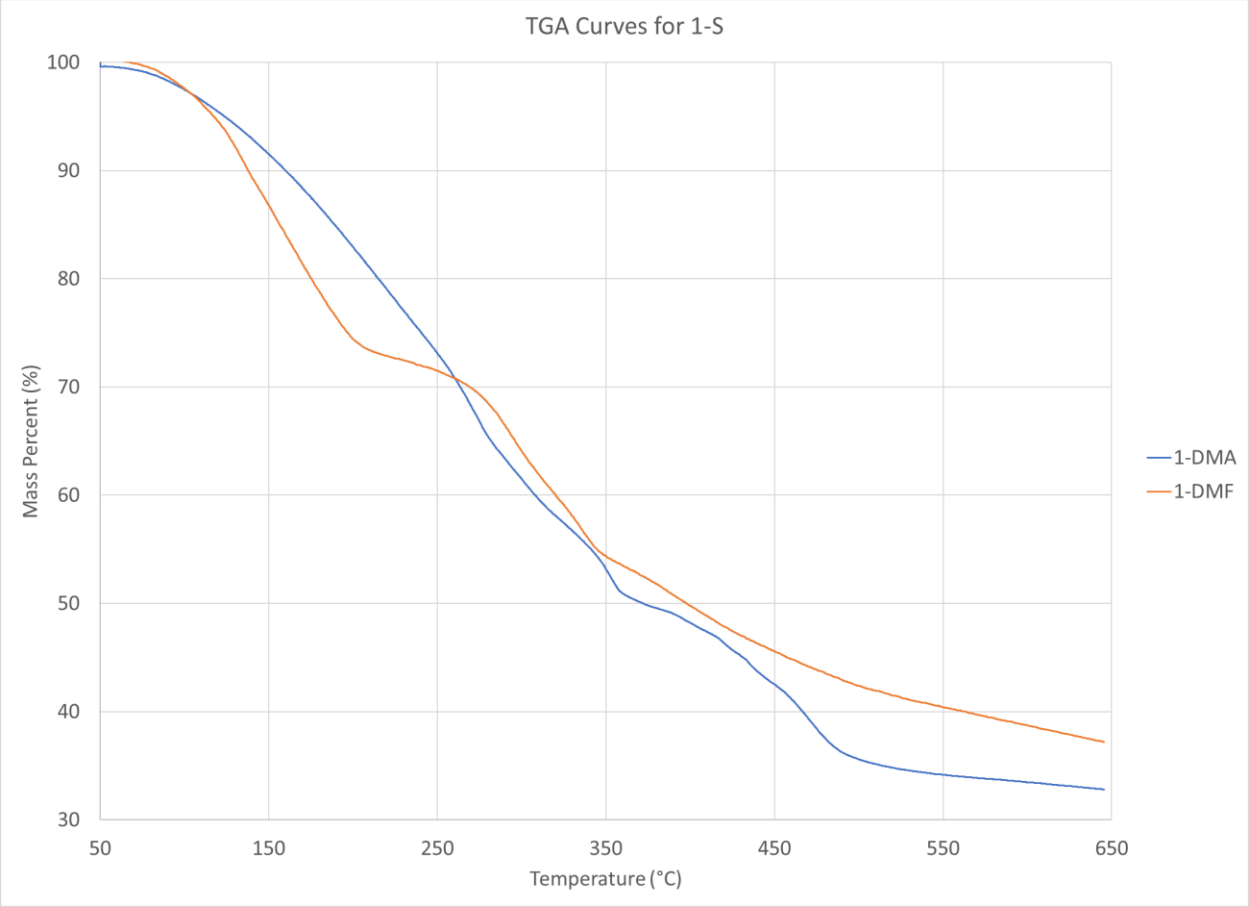

Figure S34 TGA curves for **1**-DMA and **1**-DMF

H. Gas Sorption Isotherms

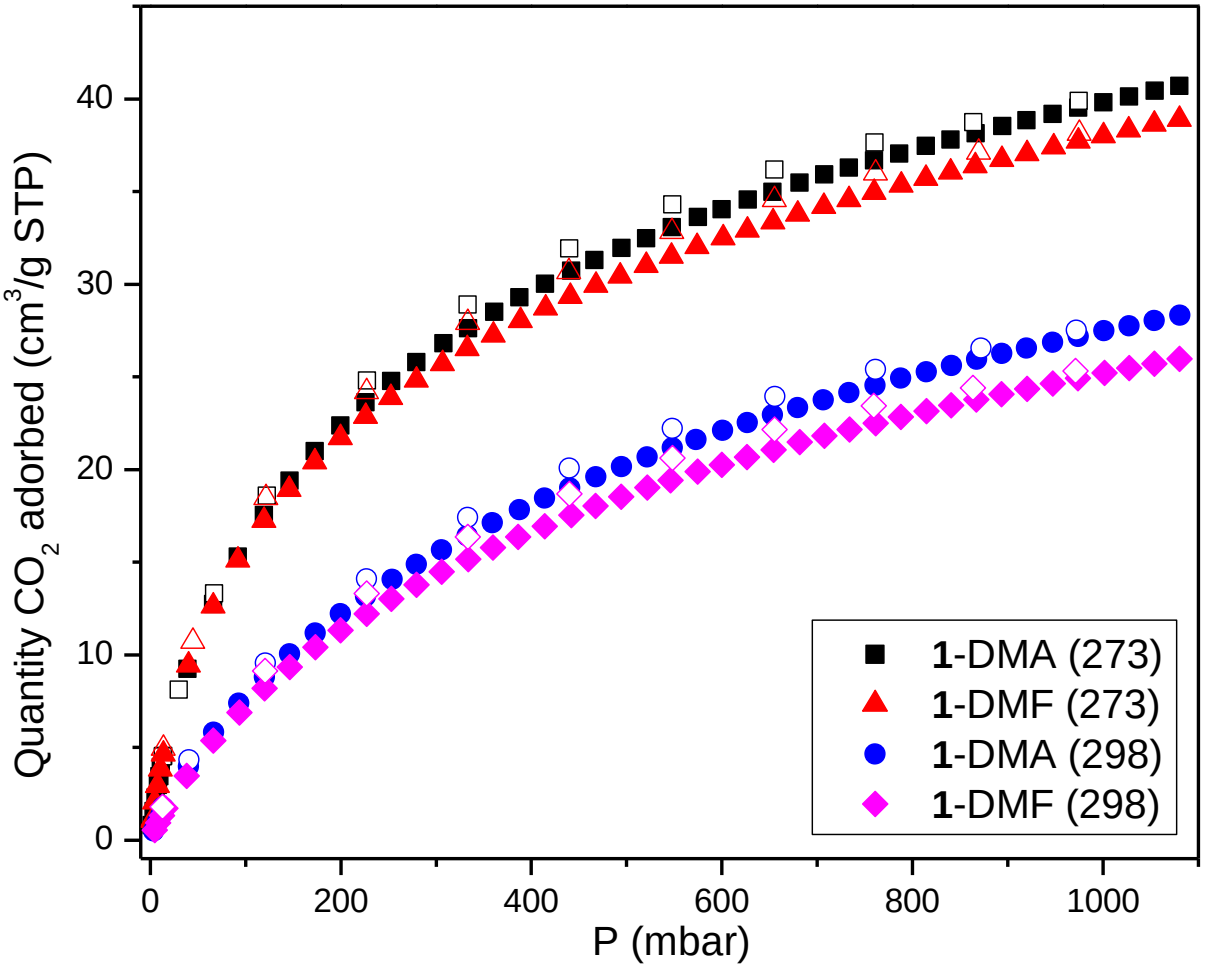

Figure S35 CO_2 sorption isotherms for **1**-DMA and **1**-DMF at 273 K and 298 K. Full symbols = adsorption, empty symbols = desorption

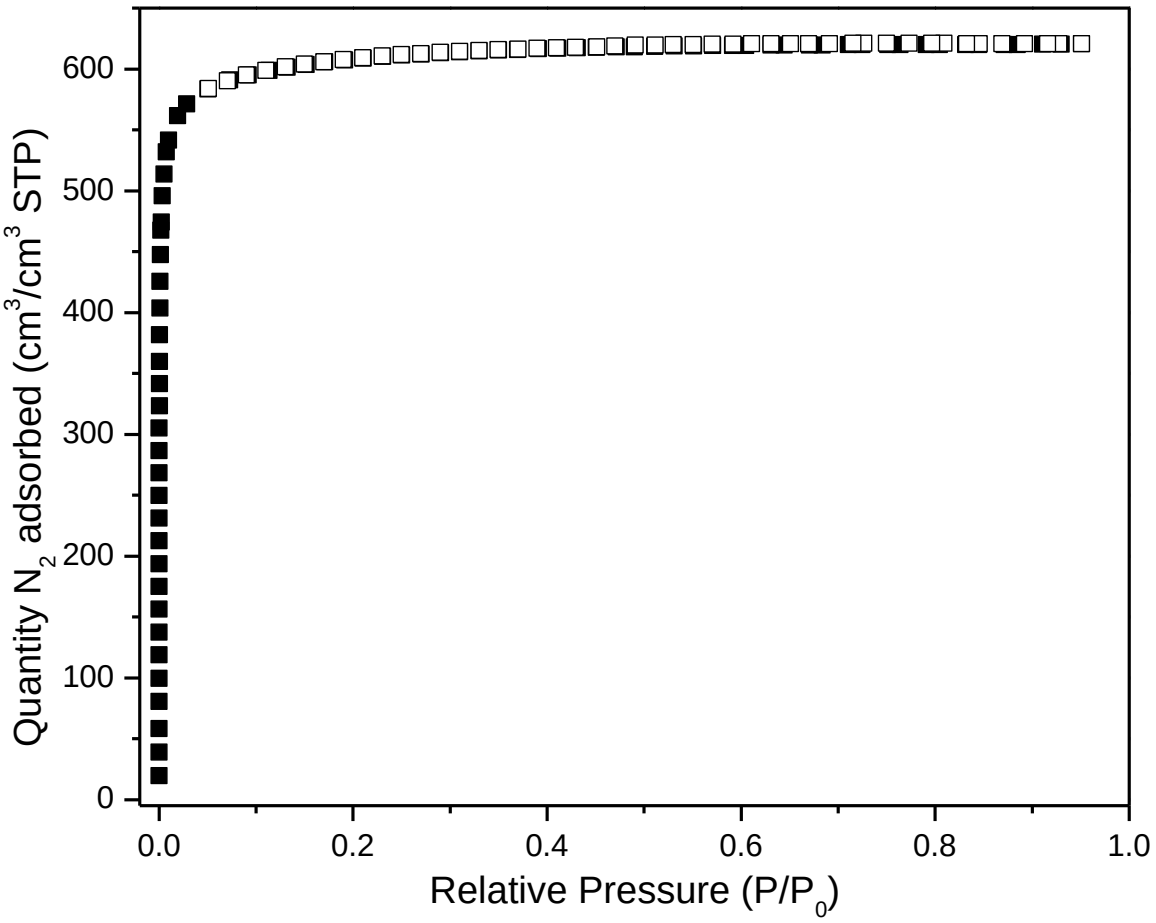

Figure S36 N_2 sorption isotherms for ZJU-105 at 77 K. Full symbols = adsorption, empty symbols = desorption. ZJU-105 was activated according to Ref 1.

I. Infrared Spectra

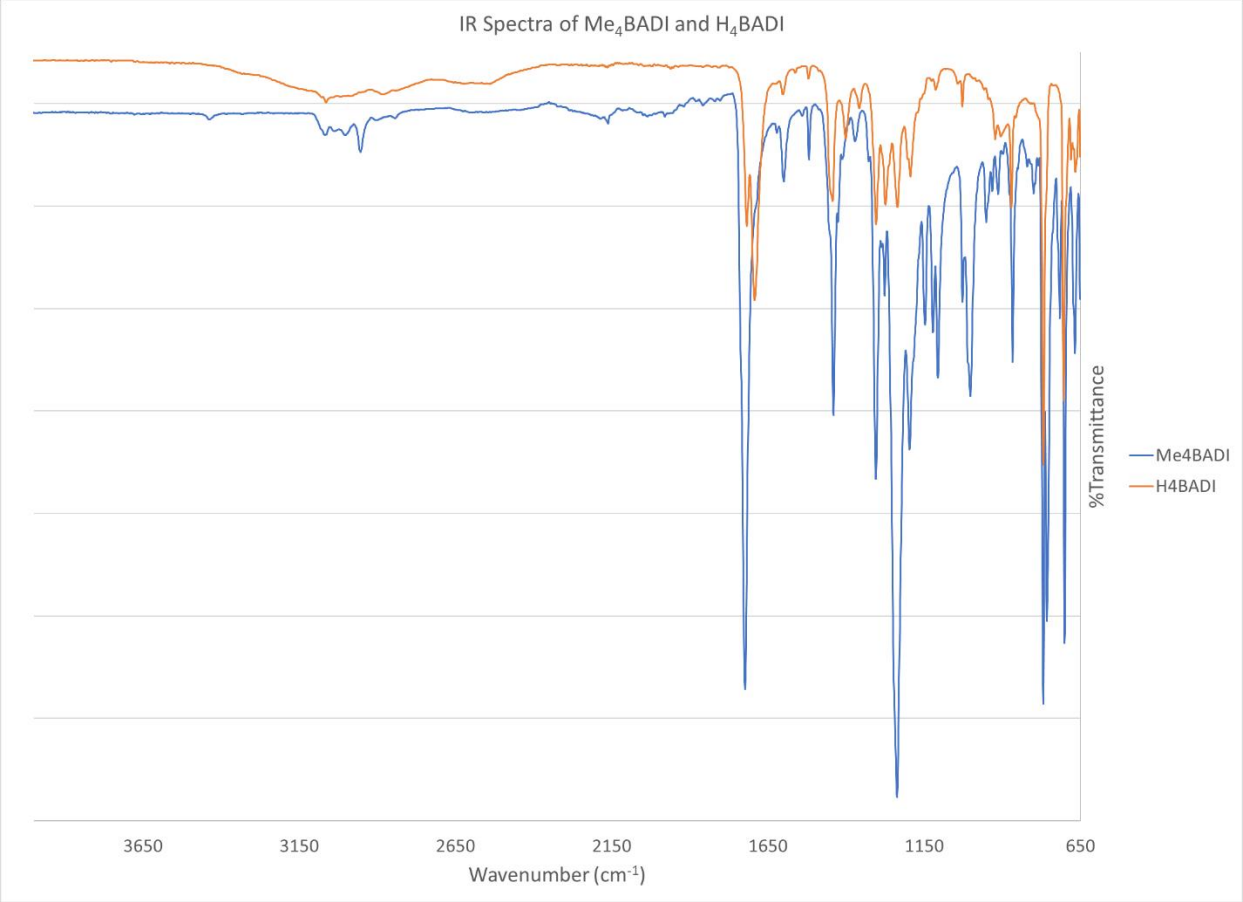

Figure S37 Infrared spectra of Me_4BADI and H_4BADI

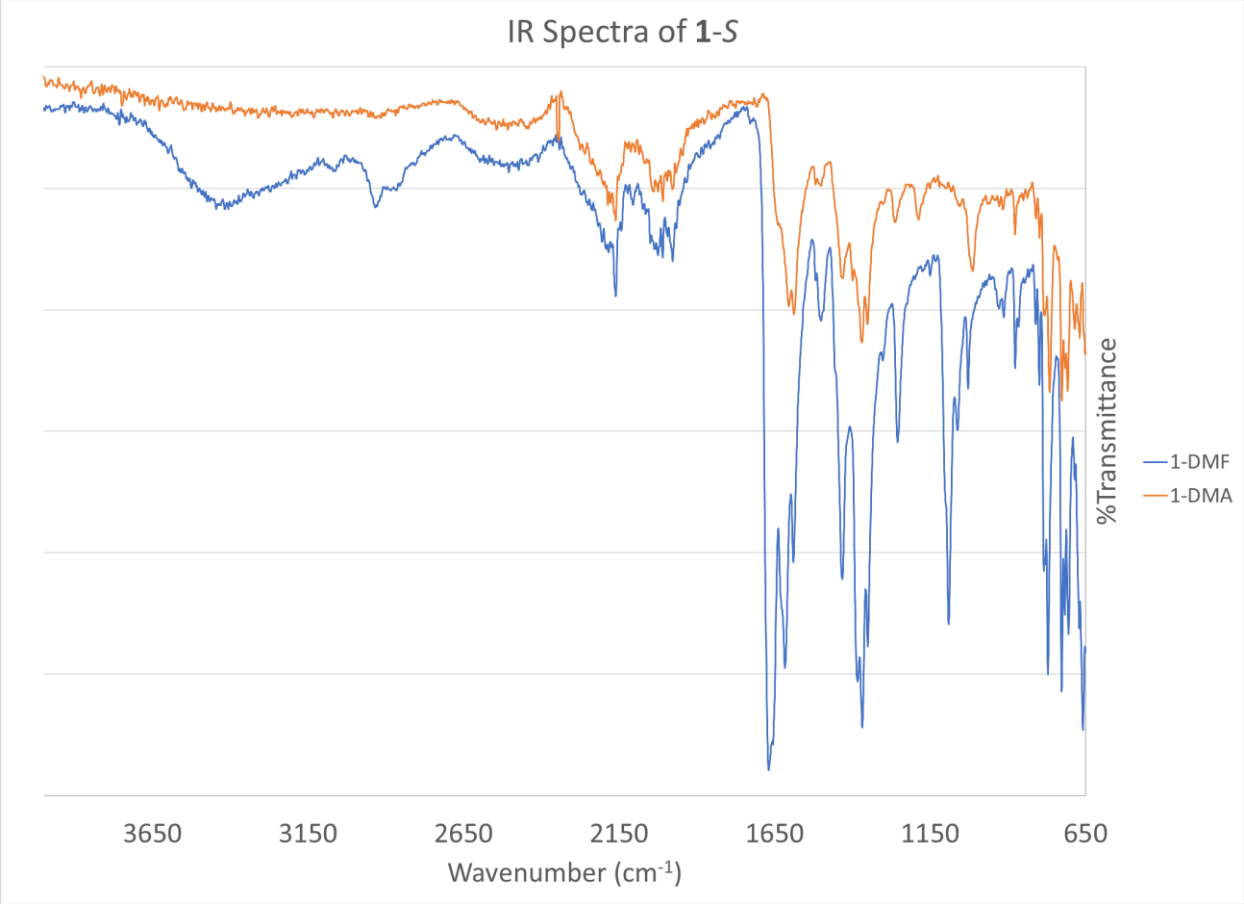

Figure S38 Infrared spectra of **1**-DMA and **1**-DMF

J. References

1. K. Shao, J. Pei, J.-X. Wang, Y. Yang, Y. Cui, W. Zhou, T. Yildirim, B. Li, B. Chen and G. Qian, *Chem. Commun.*, 2019, **55**, 11402-11405.
2. J. Jiao, H. Liu, D. Bai and Y. He, *Inorg. Chem.*, 2016, **55**, 3974-3979.
3. G. Ricciardi, A. Rosa, G. Morelli and F. Lelj, *Polyhedron*, 1991, **10**, 955-961.
4. T. Chen, J.-H. Dou, L. Yang, C. Sun, N. J. Libretto, G. Skorupskii, J. T. Miller and M. Dincă, *J. Am. Chem. Soc.*, 2020, **142**, 12367-12373.
5. Q. Jiang, P. Xiong, J. Liu, Z. Xie, Q. Wang, X.-Q. Yang, E. Hu, Y. Cao, J. Sun, Y. Xu and L. Chen, *Angew. Chem. Int. Ed.*, 2020, **59**, 5273-5277.
6. M. G. Campbell, D. Sheberla, S. F. Liu, T. M. Swager and M. Dincă, *Angew. Chem. Int. Ed.*, 2015, **54**, 4349-4352.
7. J. Muzart, *Tetrahedron*, 2009, **65**, 8313-8323.
8. J. L. Bras and J. Muzart, in *Solvents as Reagents in Organic Synthesis*, ed. X.-F. W. Wu, 2017, DOI: https://doi.org/10.1002/9783527805624.ch6, pp. 199-314.
9. Y. Jiang, I. Oh, S. H. Joo, Y.-S. Seo, S. H. Lee, W. K. Seong, Y. J. Kim, J. Hwang, S. K. Kwak, J.-W. Yoo and R. S. Ruoff, *J. Am. Chem. Soc.*, 2020, **142**, 18346-18354.
10. CrysAlisPro Software System, v1.171.42.xx, R. O. Diffraction, **2022**, Rigaku Corporation, Oxford, UK.
11. G. M. Sheldrick, *Acta Cryst. A*, 2015, **71**, 3-8.
12. G. M. Sheldrick, *Acta Cryst. C*, 2015, **71**, 3-8.
13. O. V. Dolomanov, L. J. Bourhis, R. J. Gildea, J. A. K. Howard and H. Puschmann, *J. Appl. Crystallogr.*, 2009, **42**, 339-341.
14. C. F. Macrae, I. Sovago, S. J. Cottrell, P. T. A. Galek, P. McCabe, E. Pidcock, M. Platings, G. P. Shields, J. S. Stevens, M. Towler and P. A. Wood, *J. Appl. Crystallogr.*, 2020, **53**, 226-235.
15. X. Lin, I. Telepeni, A. J. Blake, A. Dailly, C. M. Brown, J. M. Simmons, M. Zoppi, G. S. Walker, K. M. Thomas, T. J. Mays, P. Hubberstey, N. R. Champness and M. Schröder, *J. Am. Chem. Soc.*, 2009, **131**, 2159-2171.
16. J. Zhao, R. Lin, W. Tian, X. Zhu, X. Luo and Y. Liu, *Cryst. Growth Des.*, 2023, **23**, 4417-4423.
17. S. Ma, D. Sun, J. M. Simmons, C. D. Collier, D. Yuan and H.-C. Zhou, *J. Am. Chem. Soc.*, 2008, **130**, 1012-1016.
18. T. A. Makal, W. Zhuang and H.-C. Zhou, *J. Mater. Chem. A*, 2013, **1**, 13502-13509.
19. D. Sun, Y. Ke, T. M. Mattox, B. A. Ooro and H.-C. Zhou, *Chem. Commun.*, 2005, 5447-5449.